Bounding the Higgs width at the LHC

John Campbell, Fermilab

with C. Williams, K. Ellis;
1107.5569, 1311.3589, 1312.1628

Higgs properties

- Discovery of a Higgs boson in 2012 a landmark moment.
- After pinning down its mass, many questions still to answer.
  CP, spin, width, couplings to Standard Model particles: all up for grabs.

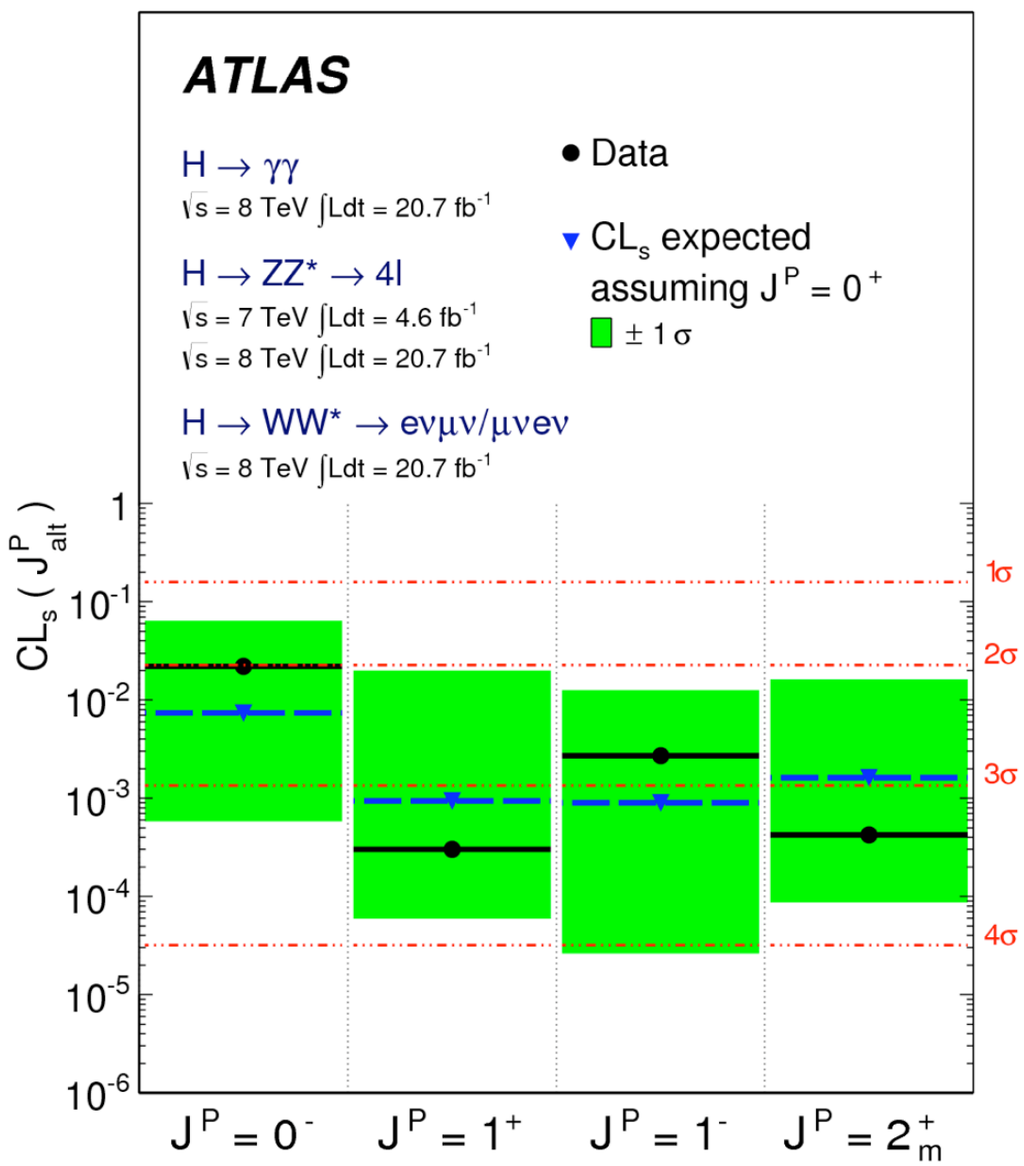

ATLAS: 1307.1432

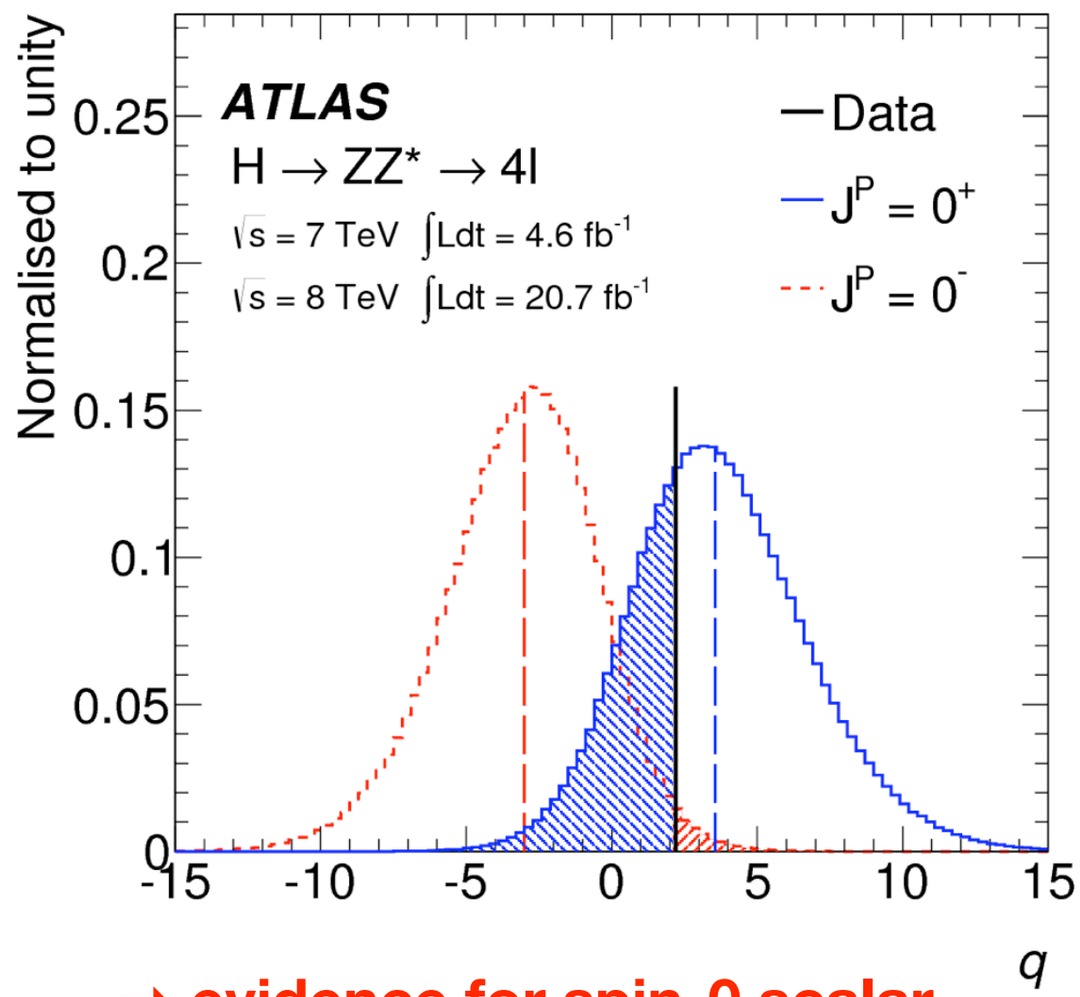

→ **evidence for spin-0 scalar**

Higgs couplings

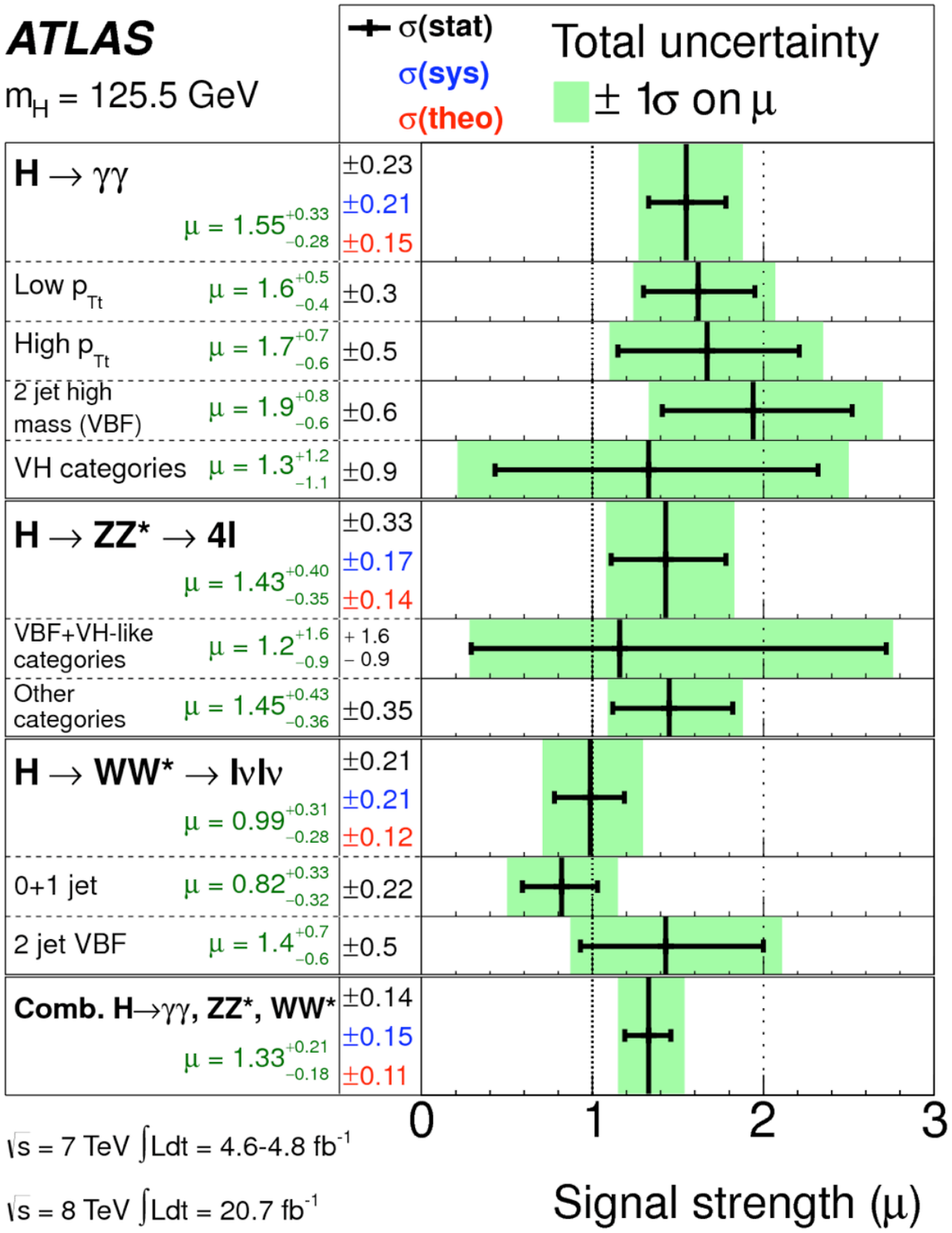

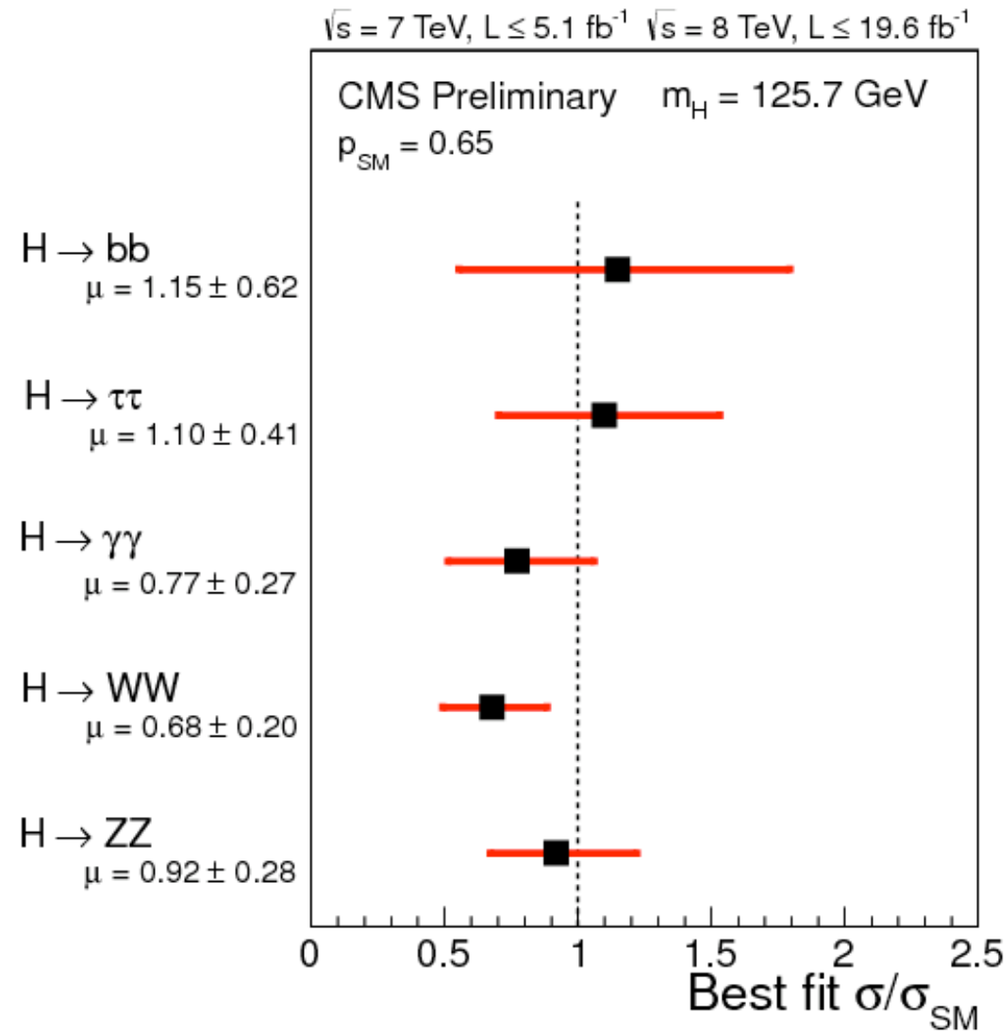

- ATLAS and CMS constrain signal strength μ, based on expected number of events relative to SM expectation.

Cross sections

- What is the theoretical expectation for the Higgs cross section?

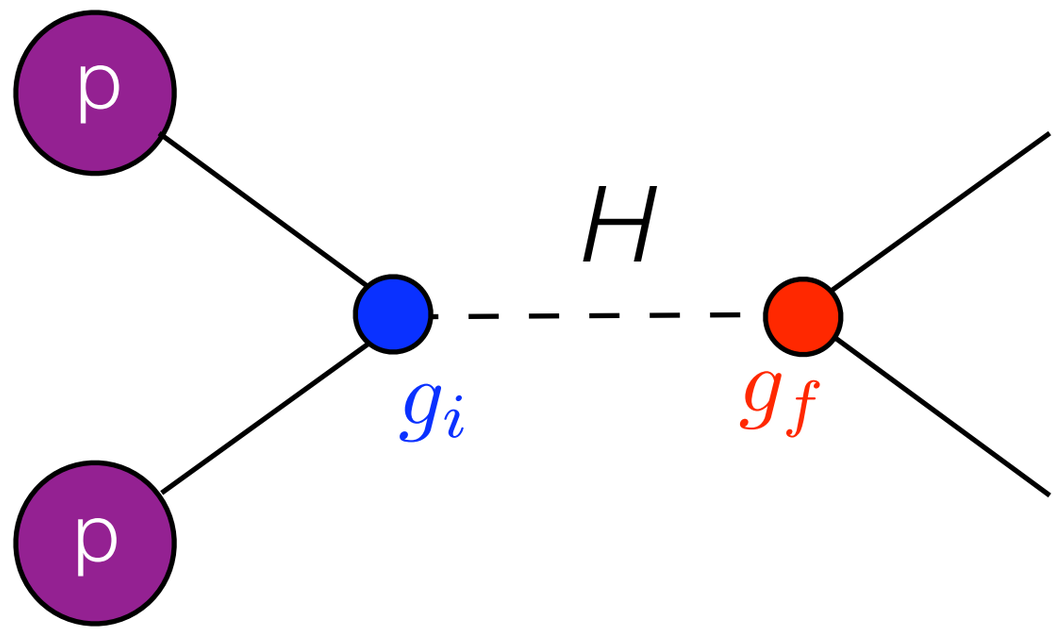

with the coupling of the Higgs boson in production and decay stages g_i and g_f.

- Total cross section depends not only on the strengths of these couplings, but also on the width of the resonance:

$$\sigma_{i \to H \to f} \sim \frac{g_i^2 \, g_f^2}{\Gamma_H}$$

- Can we determine the width and untangle the dependence?

Higgs width - how large?

- Predicted in the Standard Model: sum over partial widths into known channels.
- Below vector boson pair threshold, dominated by decay into b-quarks.

$$\Gamma_H \approx \Gamma(H \to b\bar{b}) \approx \frac{N_c g_w^2 m_b^2 m_H}{32\pi m_W^2} = \mathcal{O}(\mathrm{MeV}) \quad \text{for } m_H \lesssim 140 \text{ GeV}$$

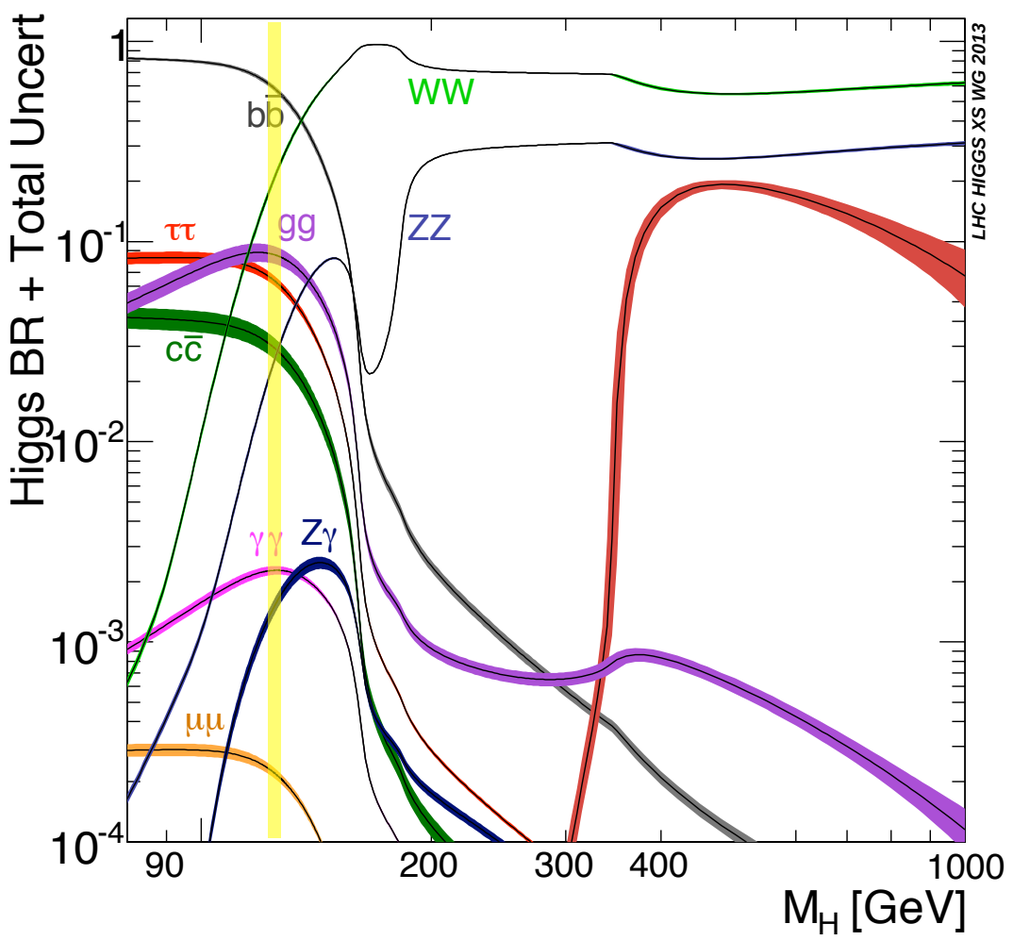

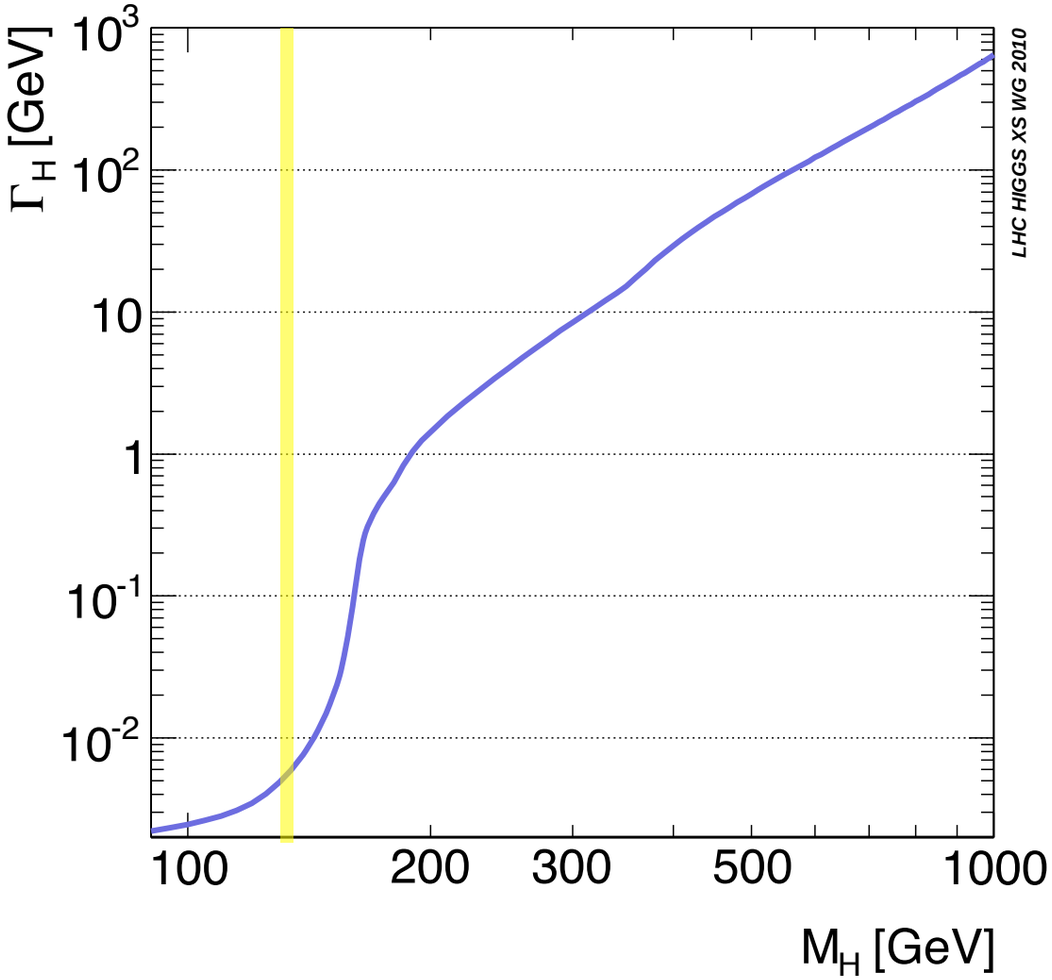

Current constraints

- How can we probe a width of a few MeV at the LHC?

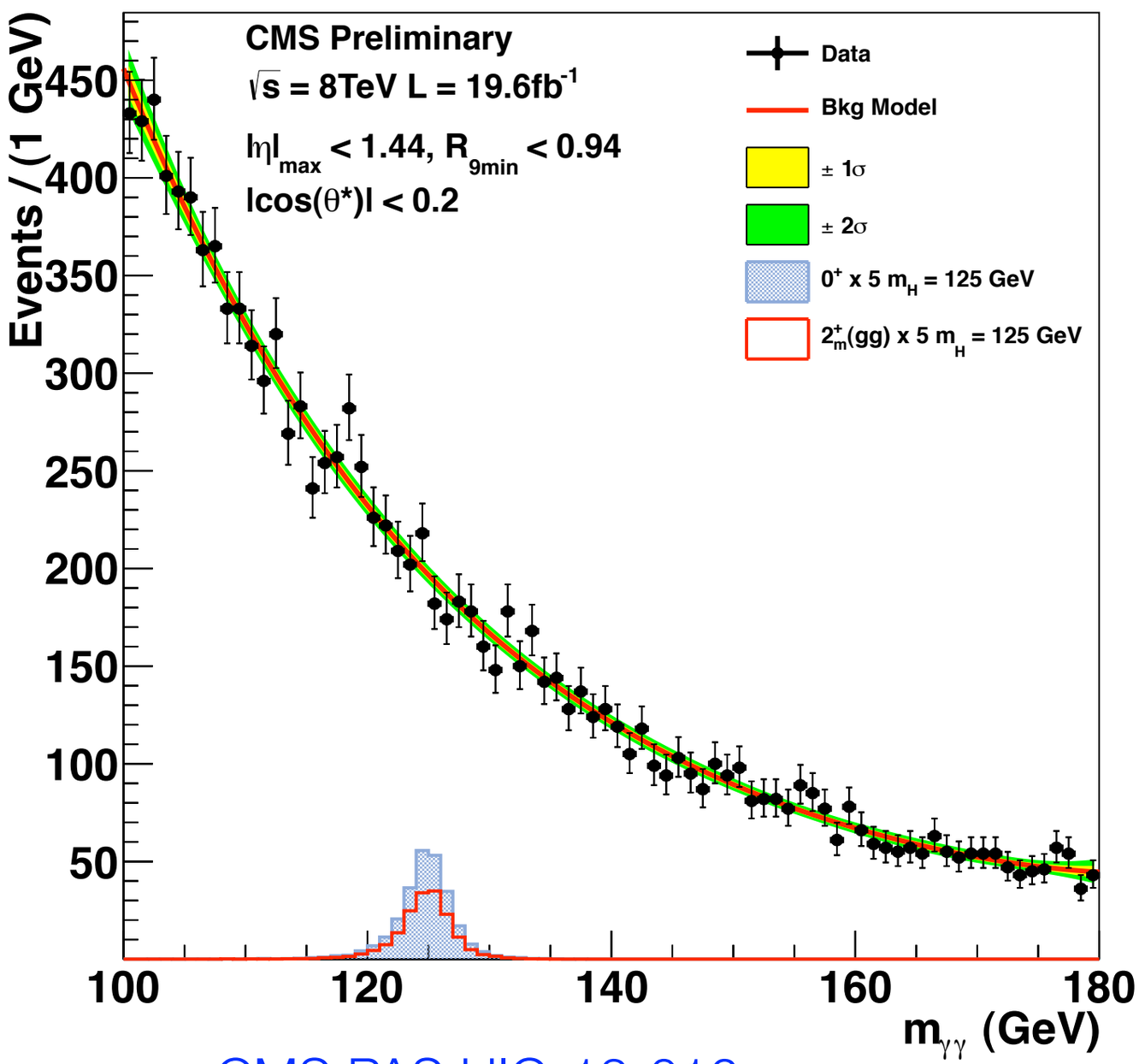

CMS PAS HIG-13-016

- Intrinsic detector resolution is of order a few GeV in the most well-measured channels.
- Direct limits inherently weak:

$$\Gamma_H < 6.9 \text{ GeV}$$

$$(95\% \text{ confidence})$$

$$\left(\Gamma_H \lesssim 1600\, \Gamma_H^{\rm SM}\right)$$

- Assume bound scales with statistics, combine with ZZ channel, 3000 fb^{-1}:

$$\Gamma_H \lesssim 200 \text{ MeV} \quad \left(\sim 50\, \Gamma_H^{\rm SM}\right)$$

Future lepton colliders

- The width of the Higgs boson is a key deliverable of future lepton colliders.
- Clear strategy for an ILC.

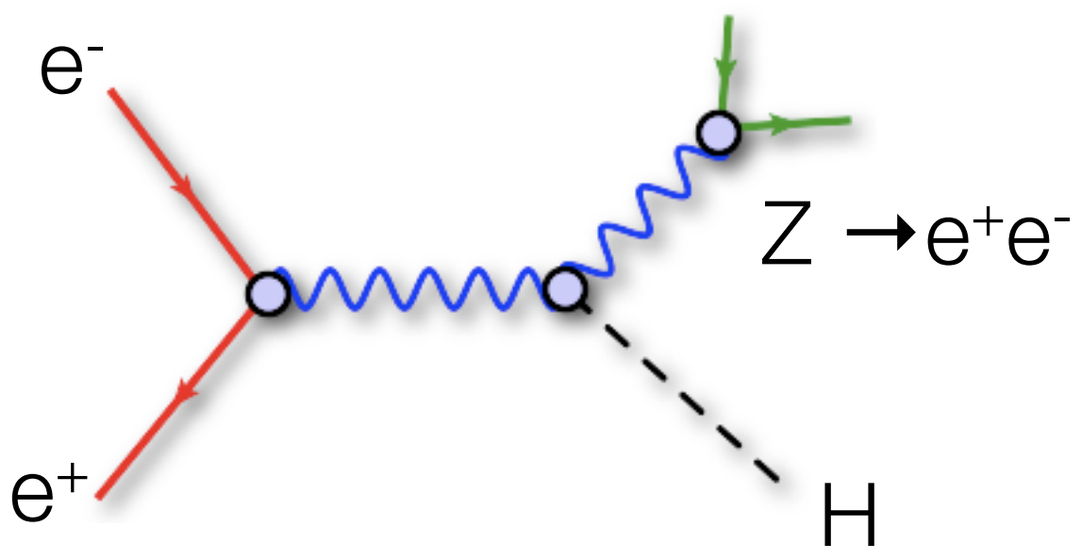

- Tag ZH events where recoil mass is consistent with a Higgs boson → measurement of σ(ZH)
- Measurement of H→ZZ rate then determines Br(H→ZZ)

$$\Gamma_H = \Gamma(H \to ZZ)/\mathrm{Br}(H \to ZZ) \propto \sigma(ZH)/\mathrm{Br}(H \to ZZ)$$

- At 350 GeV and beyond (CLIC/TLEP), similar analysis through WW fusion.

Facility	ILC			ILC(LumiUp)	TLEP (4 IP)		CLIC		
$\sqrt{s}$ (GeV)	250	500	1000	250/500/1000	240	350	350	1400	3000
$\int \mathcal{L}dt$ (fb^{-1})	250	+500	+1000	1150+1600+2500‡	10000	+2600	500	+1500	+2000
$P(e^-, e^+)$	$(-0.8, +0.3)$	$(-0.8, +0.3)$	$(-0.8, +0.2)$	(same)	$(0, 0)$	$(0, 0)$	$(0, 0)$	$(-0.8, 0)$	$(-0.8, 0)$
Γ_H	12%	5.0%	4.6%	2.5%	1.9%	1.0%	9.2%	8.5%	8.4%

1%-10% precision

Snowmass Higgs WG,1310.8361

Future lepton colliders

- Muon collider: direct scan of Higgs threshold.
- Biggest systematic uncertainty from knowledge of muon beam.

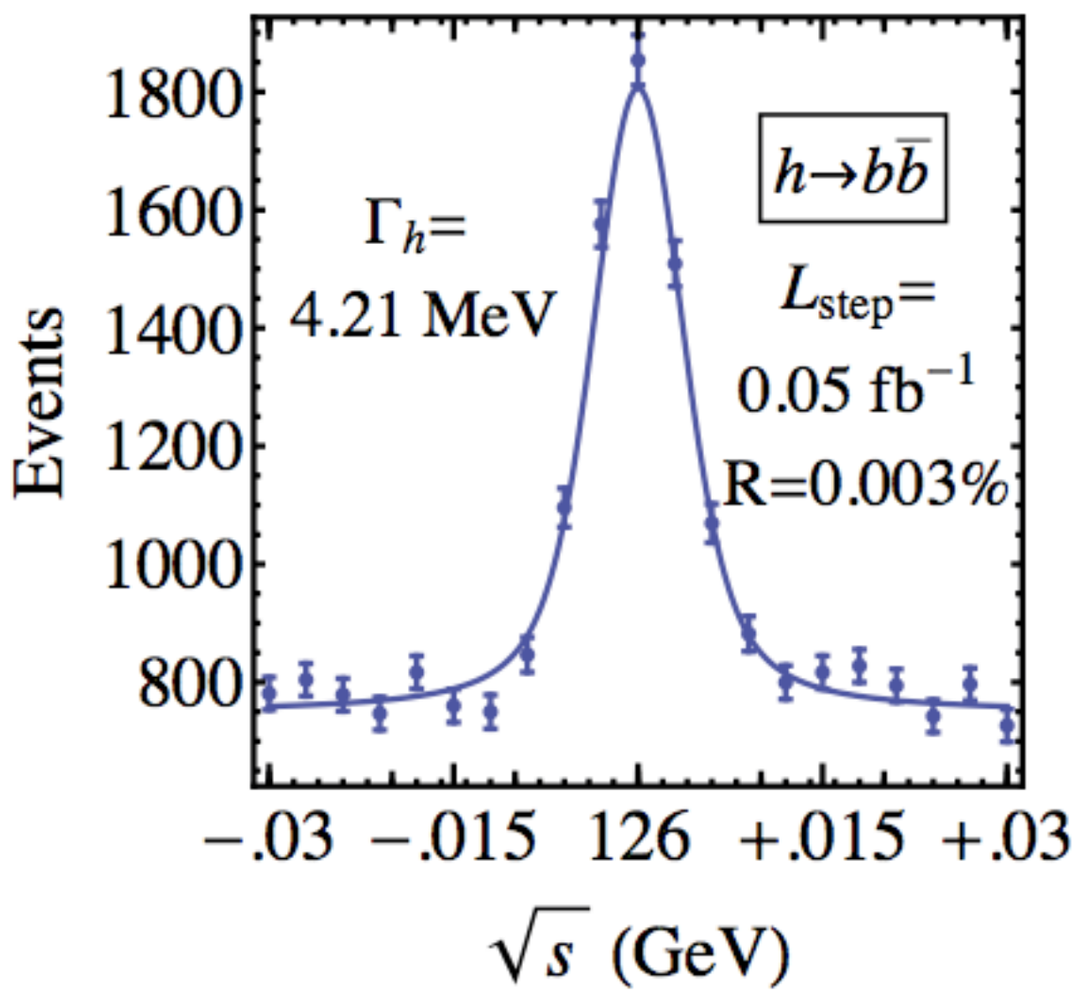

Muon collider Higgs factory study,1308.2143

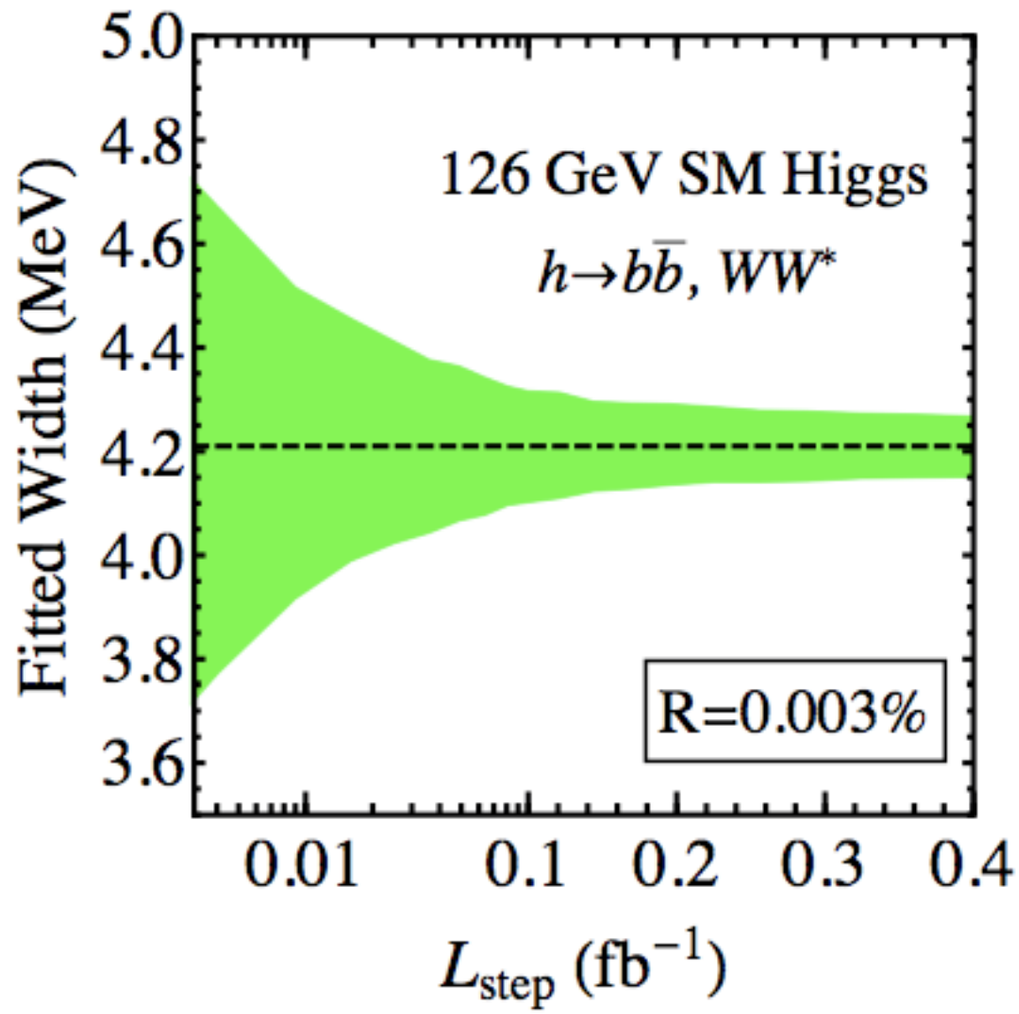

~5% precision

Sketch of Caola-Melnikov method (essence of 1307.4935)

- Consider the Drell-Yan process. Can map out the resonance as a function of the four-momentum squared (s) that appears in the propagator.

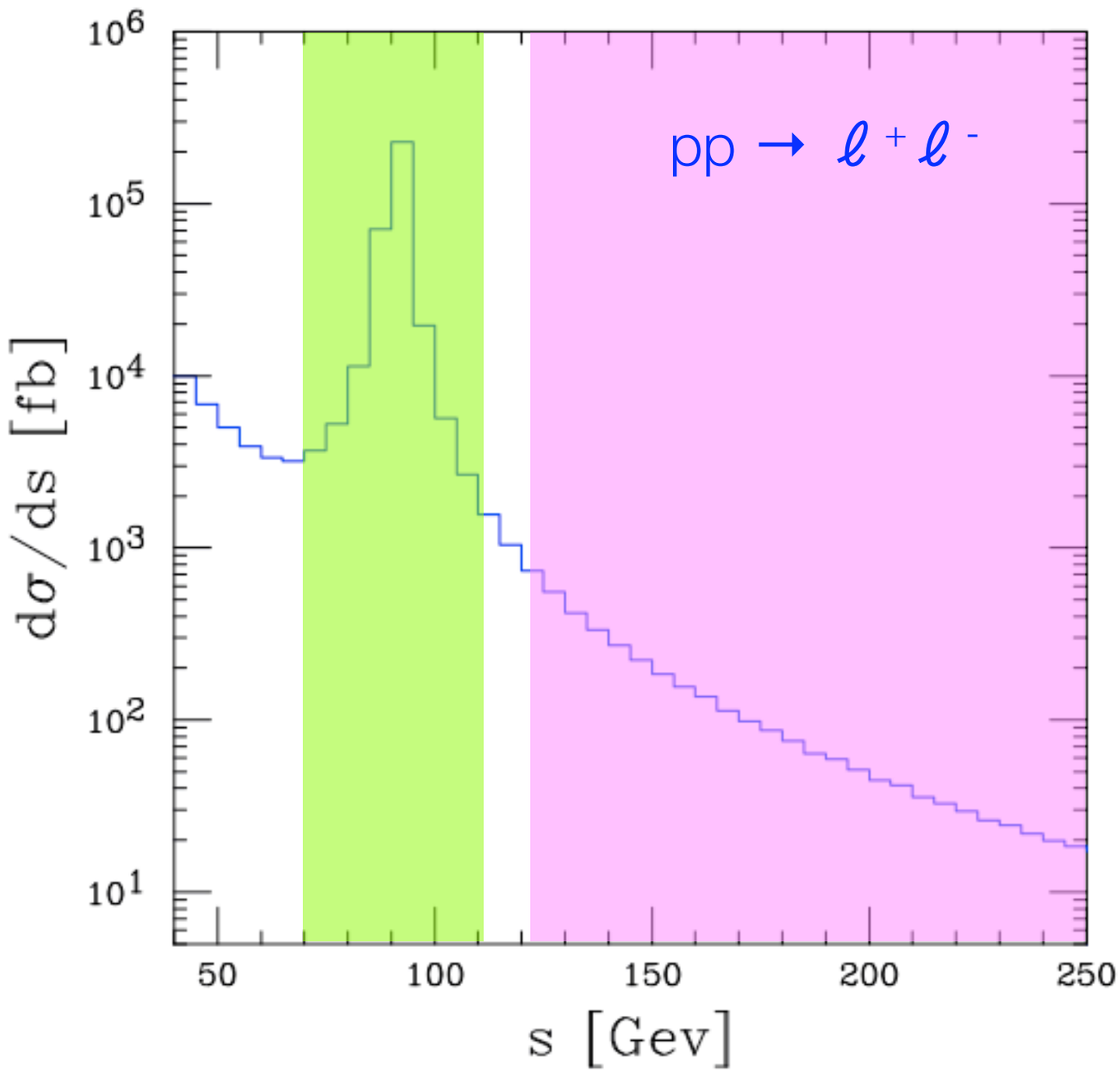

- "On-shell" cross section in resonance region:

$$\sigma_{\rm on} \sim \int \frac{{\rm d}s}{(s-m_Z^2)^2+\Gamma_Z^2 m_Z^2} \propto \frac{1}{\Gamma_Z}$$

- "Off-shell" cross section above the resonance:

$$\sigma_{\rm off} \sim \int_{s \gg m_Z^2} \frac{{\rm d}s}{(s-m_Z^2)^2+\cancel{\Gamma_Z^2 m_Z^2}}$$

(approx.) independent of width.

- Form ratio:

$$\Gamma \propto \frac{\sigma_{\rm off}}{\sigma_{\rm on}}$$

How does it work for the Higgs boson?

- Naive expectation: $\Gamma_H / m_H \sim 10^{-5}$; resonance peak so narrow that there is no off-shell cross section to measure.
- This is spectacularly wrong for the golden channel.

$$p + p \to H \to ZZ$$
$$\hookrightarrow \mu^- + \mu^+$$
$$\hookrightarrow e^- + e^+ .$$

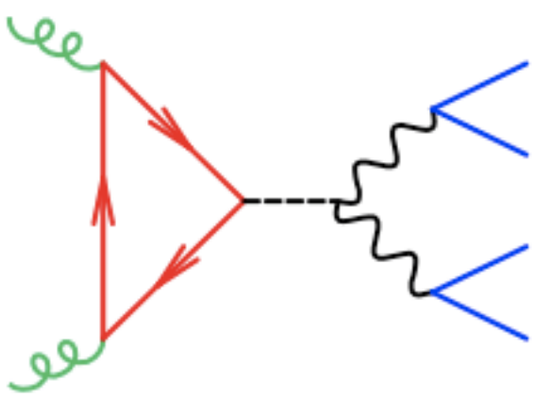

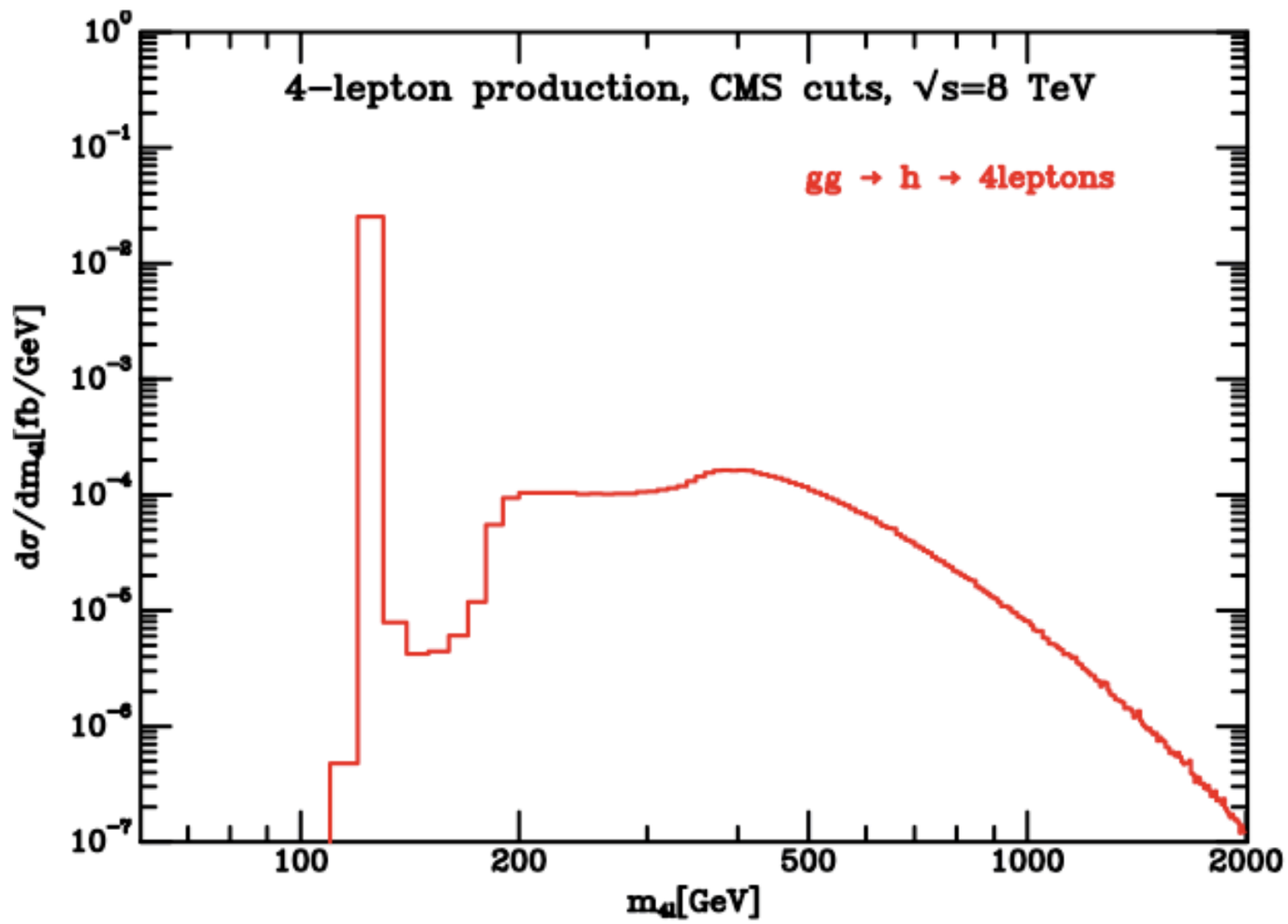

- About 15% of the total cross section in the region with $m_{4\ell} > 130$ GeV.

  Kauer, Passarino,1206.4803

Ingredients

- In order to assess viability of an analysis based on this fact, need precision prediction for the 4-lepton final state.

$(a): g(-p_1) + g(-p_2) \to H \to e^-(p_3) + e^+(p_4) + \mu^-(p_5) + \mu^+(p_6)$	$O(g_s^2 e^4)$
$(b): g(-p_1) + g(-p_2) \to e^-(p_3) + e^+(p_4) + \mu^-(p_5) + \mu^+(p_6)$	$O(g_s^2 e^4)$
$(c): q(-p_1) + \bar{q}(-p_2) \to e^-(p_3) + e^+(p_4) + \mu^-(p_5) + \mu^+(p_6)$	$O(e^4)$
$(d): q(-p_1) + g(-p_2) \to H \to e^-(p_3) + e^+(p_4) + \mu^-(p_5) + \mu^+(p_6) + q(p_7)$	$O(g_s^3 e^4)$
$(e): q(-p_1) + g(-p_2) \to e^-(p_3) + e^+(p_4) + \mu^-(p_5) + \mu^+(p_6) + q(p_7)$	$O(g_s e^4)$

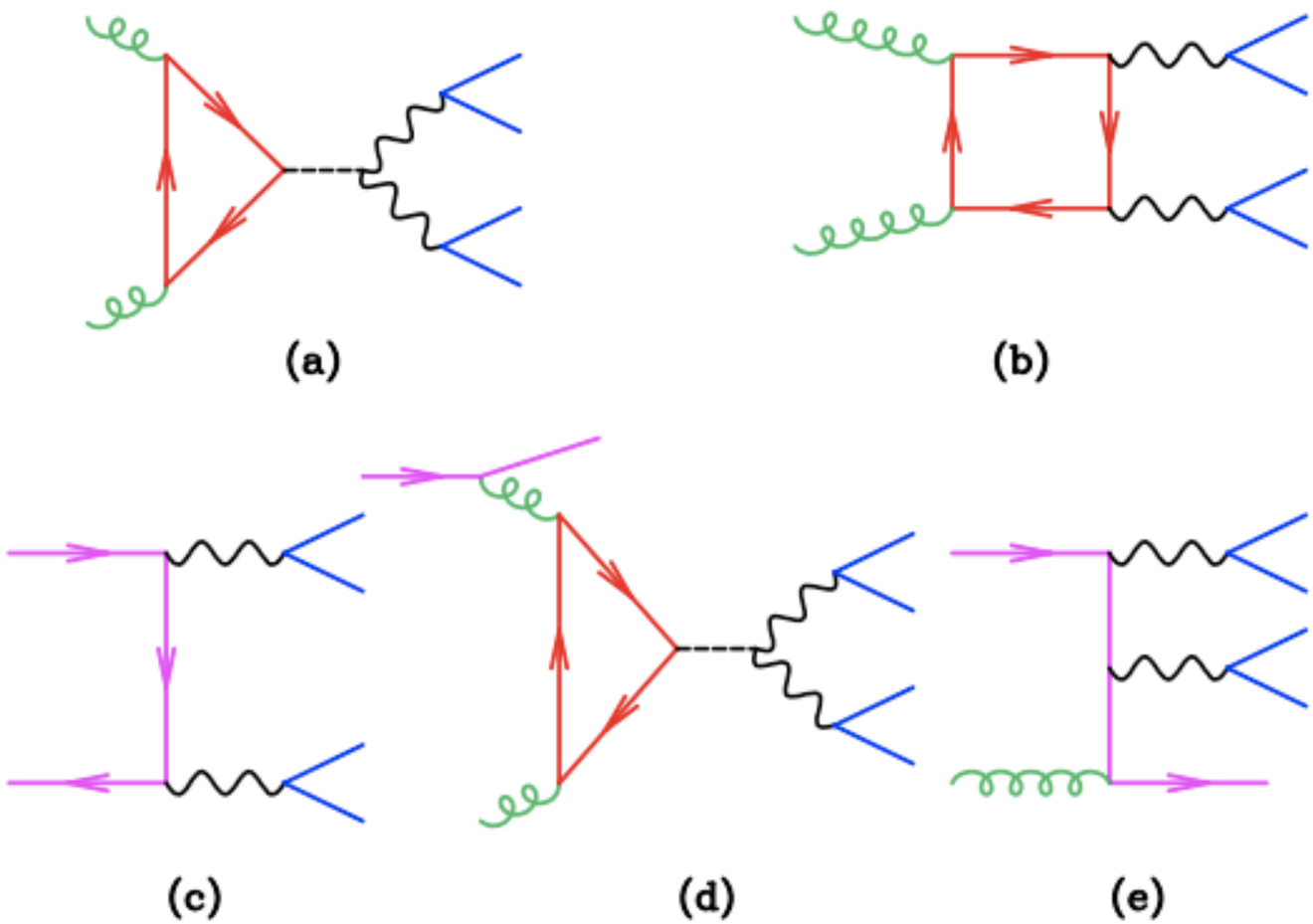

(a)+(b): gluon initiated (signal and background)

(c): dominant background

(d)+(e): “qg interference”, same order as (a)*(b)

Importance of interference

- Usual classification into “signal” and “background” contributions neglects the effect of interference
  - that is particularly important since a Higgs boson is involved.
- Consider high-energy $t\bar{t} \to ZZ$ scattering (diagrams embedded in loops).
  - straightforward to examine behavior using longitudinal modes of Z’s

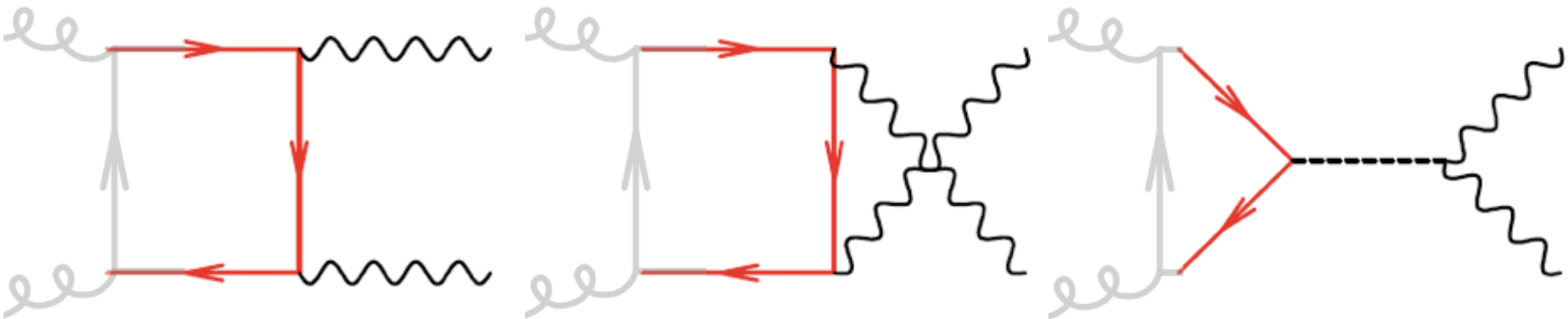

$aE^2 + (b+c)m_t E$ $\quad$ $-aE^2 + (d-c)m_t E$ $\quad$ $-(b+d)m_t E$

- Inclusion of Higgs diagram essential to cancel bad high energy behaviour.
- An observation of this mechanism at work would be evidence of the Higgs boson doing its job.

Calculation

- Most contributions are either tree-level or simple 3-point diagrams.
- Most challenging calculation is the gg→ZZ box diagrams.
- Only six basic diagrams; contract with Z currents later.

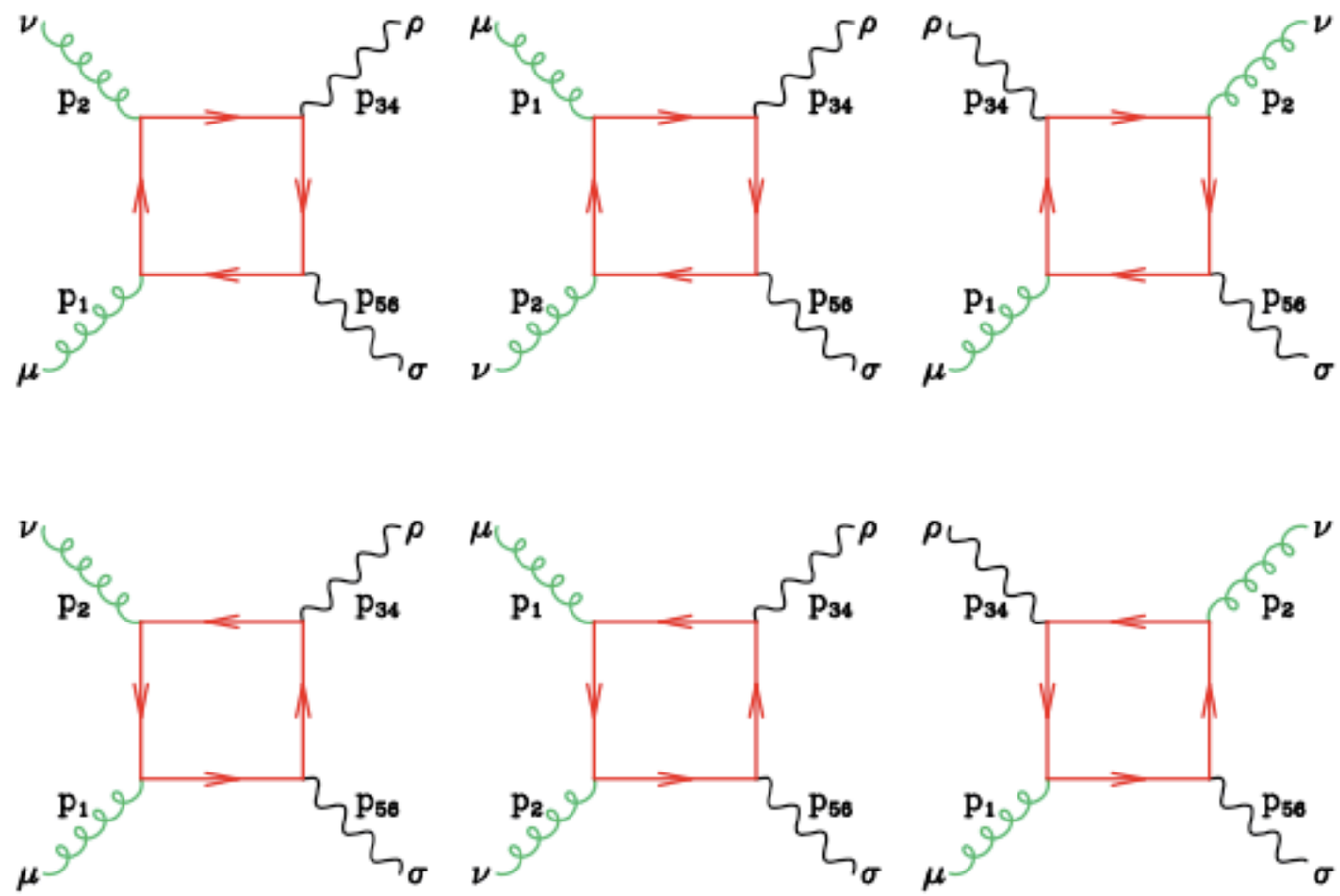

- As we've seen, essential to account for quark masses in the loop.
- Classify contributions according to couplings of the Z's to quarks. Mixed vector(V)/axial(A) contribution vanishes, so two independent contributions: either (VV,AA), or in terms of left(L) and right(R) -handed couplings (LL,LR)

$$A_{VV} = 2\left(A_{LL} + A_{LR}\right) \ , \qquad A_{AA} = 2\left(A_{LL} - A_{LR}\right)$$

History

- A long and rich history with some local flavour.
- VV amplitude calculated in 1971 using a dispersive technique.
  Constantini, de Tollis, Pistoni; Nuovo Cim. A2 (1971)
- LR amplitudes in 1989, for strictly on-shell Z's.
  Glover, van der Bij; NPB 321 (1989)
- Extension to off-shell Z-bosons.
  Zecher et al; hep-ph/9404295
- Numerical calculation including leptonic decays.
  Binoth, Kauer, Mertsch; 0807.0024
- Analytic form of amplitudes for massless quarks (only VV relevant).
  Bern, Dixon, Kosower; hep-ph/9708239
- Implementation of all contributions (numerically) in gg2VV code.
  Kauer, Passarino; 1206.4806
- Aim: full analytic calculation for fast and numerically stable evaluation.

LR amplitude

- Hard to improve on the treatment of Glover and van der Bij; small extension to off-shell Z-bosons.
- Result is manifestly gauge invariant wrt. the gluons (indices μ and ν):

$$
\begin{aligned}
P_{LR}^{\mu\nu\rho\sigma} &= A_1\, g^{\rho\sigma}\Big(g^{\mu\nu} - \frac{p_1^\nu p_2^\mu}{p_1\cdot p_2}\Big) \\
&+ A_2\, g^{\rho\sigma}\Big(g^{\mu\nu} + \frac{2}{p_T^2}p_{34}^\mu p_{34}^\nu + \frac{p_{34}^2}{p_T^2 p_1\cdot p_2}p_1^\nu p_2^\mu - \frac{2p_1\cdot p_{34}}{p_T^2 p_1\cdot p_2}p_2^\mu p_{34}^\nu - \frac{2p_2\cdot p_{34}}{p_T^2 p_1\cdot p_2}p_1^\nu p_{34}^\mu\Big) \\
&+ A_3\Big(g^{\mu\sigma}g^{\nu\rho} + \frac{g^{\mu\nu}p_1^\sigma p_2^\rho}{p_1\cdot p_2} - \frac{g^{\nu\rho}p_1^\sigma p_2^\mu}{p_1\cdot p_2} - \frac{g^{\mu\sigma}p_1^\nu p_2^\rho}{p_1\cdot p_2}\Big) \\
&+ A_4\Big(g^{\mu\rho}g^{\nu\sigma} + \frac{g^{\mu\nu}p_1^\rho p_2^\sigma}{p_1\cdot p_2} - \frac{g^{\nu\sigma}p_1^\rho p_2^\mu}{p_1\cdot p_2} - \frac{g^{\mu\rho}p_1^\nu p_2^\sigma}{p_1\cdot p_2}\Big) \\
&+ A_5\,\frac{1}{p_1\cdot p_2}\Big(g^{\mu\sigma}p_1^\rho p_{34}^\sigma - g^{\mu\rho}p_1^\sigma p_{34}^\nu + g^{\nu\sigma}p_2^\rho p_{34}^\mu - g^{\nu\rho}p_2^\sigma p_{34}^\mu \\
&+ \frac{p_2\cdot p_{34}}{p_1\cdot p_2}g^{\mu\rho}p_1^\nu p_1^\sigma - \frac{p_2\cdot p_{34}}{p_1\cdot p_2}g^{\mu\sigma}p_1^\nu p_1^\rho + \frac{p_1\cdot p_{34}}{p_1\cdot p_2}g^{\nu\rho}p_2^\mu p_2^\sigma - \frac{p_1\cdot p_{34}}{p_1\cdot p_2}g^{\nu\sigma}p_2^\mu p_2^\rho\Big) \\
&+ A_6\,\frac{1}{p_1\cdot p_2}\Big(g^{\mu\sigma}p_1^\rho p_{34}^\nu - g^{\mu\rho}p_1^\sigma p_{34}^\nu + g^{\mu\rho}p_1^\nu p_1^\sigma\frac{p_2\cdot p_{34}}{p_1\cdot p_2} - g^{\mu\sigma}p_1^\nu p_1^\rho\frac{p_2\cdot p_{34}}{p_1\cdot p_2}\Big)\,.
\end{aligned}
$$

- Contract:

$$
\begin{aligned}
A(1_g^+, 2_g^+, 3_e^-, 4_{\bar e}^+, 5_\mu^-, 6_{\bar\mu}^+) &= \frac{1}{s_{12}s_{34}s_{56}}\frac{\langle 3\,5\rangle}{\langle 1\,2\rangle}\Big[[1\,6][4\,2]s_{12}\,(A_3 + A_1) - [2\,6][4\,1]s_{12}\,(A_4 + A_1) \\
&+ \Big([2\,4][2\,6]\langle 2|(3+4)|1] - [1\,4][1\,6]\langle 1|(3+4)|2]\Big)\,A_5\Big]\,.
\end{aligned}
$$

Form factors for LR amplitude

- The functions A_1 ... A_6 collect scalar one-loop integrals.
- For example:

$D_0 \rightarrow$ box integral

$$A_5 = \frac{m^2 s}{2 s_{234} s_{134}} \Big[2 s_{134} D_0^{d=6}(3) + 2 s_{234} D_0^{d=6}(2) - s_{234} s_{134} D_0(1) + 4m^2 \Big(s_{134} D_0(3) + s_{234} D_0(2) \Big) + 2(s_{234} + s_{134}) C_0(2) \Big]$$

$C_0 \rightarrow$ triangle integral

- It is convenient to also introduce the 6-dimensional box function which can itself be written in terms of the usual 4-d scalar integrals, e.g.

$$D_0^{d=6}(2) = \frac{s_{134}}{2Y} \Big[(s_{13} + s_{14}) C_0(3) + (s_{25} + s_{26}) C_0(6) + s_{12} C_0(1) + \Big(s_{12} - s_{34} - s_{56} + 2 \frac{s_{34} s_{56}}{s_{134}} \Big) C_0(2) - \Big(s_{12} s_{134} + \frac{4m^2 Y}{s_{134}} \Big) D_0(2) \Big]$$

- Overall factor of the box Gram determinant: $Y = s_{12} p_T^2 = 4\, p_{34}.p_1\, p_{34}.p_2 - s_{12} s_{34}$
  - in the limit that $Y \rightarrow 0$, the scalar integrals combine such that $D_0^{d=6}$ is finite.

LL amplitude

- The LL amplitude is a different story: use *D*-dimensional unitarity techniques to obtain coefficients of basic integrals.

  Britto, Cachazo, Feng, hep-th/0412103; Forde, 0704.1835

- Integral basis slightly expanded to use the same 6-d boxes:

$$A_{LL}(1_g^{h_1}, 2_g^{h_2}, 3_e^-, 4_{\bar{e}}^+, 5_\mu^-, 6_{\bar{\mu}}^+) = \sum_{j=2}^{3} d_j^{d=6}(1^{h_1}, 2^{h_2})\, D_0^{d=6}(j) + \sum_{j=1}^{3} d_j(1^{h_1}, 2^{h_2})\, D_0(j) + \sum_{j=1}^{6} c_j(1^{h_1}, 2^{h_2})\, C_0(j) + \sum_{j=1}^{6} b_j(1^{h_1}, 2^{h_2})\, B_0(j) + R(1^{h_1}, 2^{h_2})$$

- Coefficients expanded as a function of mass in the loop:

$$d_i(1^{h_1}, 2^{h_2}) = d_i^{(0)}(1^{h_1}, 2^{h_2}) + m^2 d_i^{(2)}(1^{h_1}, 2^{h_2}) + m^4 d_i^{(4)}(1^{h_1}, 2^{h_2})$$
$$c_i(1^{h_1}, 2^{h_2}) = c_i^{(0)}(1^{h_1}, 2^{h_2}) + m^2 c_i^{(2)}(1^{h_1}, 2^{h_2}),$$

- $d^{(0)}$ and $c^{(0)}$ terms in coefficients already known in compact form; bubble coefficients and rational terms are independent of the mass.

- Exploit relationship between rational terms and m^2 coefficients of triangles, m^4 coefficients of boxes:

$$R(1^{h_1}, 2^{h_2}) - \frac{1}{2}\sum_{j=1}^{6} c_j^{(2)}(1^{h_1}, 2^{h_2}) + \frac{1}{6}\sum_{j=1}^{3} d_j^{(4)}(1^{h_1}, 2^{h_2}) = 0$$

Example coefficients

- Written in compact spinor notation: $\langle i\,j\rangle = \bar{u}_-(p_i)u_+(p_j), \quad [i\,j] = \bar{u}_+(p_i)u_-(p_j)$
- Typical box :

$$
\begin{aligned}
d_1^{(0)}(1^-,2^+) &= 0 \\
d_1^{(2)}(1^-,2^+) &= \Big\{\frac{1}{2}\Big[-\frac{\langle 5\,6\rangle\langle 1|(3+4)|2]\langle 3|(2+4)|1][4\,1][6\,2]^2}{\langle 2|(3+4)|1][2\,1]^2} \\
&\quad + \frac{\langle 1\,5\rangle^2\langle 2\,3\rangle\langle 1|(3+4)|2]\langle 2|(1+3)|4][6\,5]}{\langle 1\,2\rangle^2\langle 2|(3+4)|1]}\Big]\frac{1}{s_{34}s_{56}}\Big\} + \Big\{3\leftrightarrow 5, 4\leftrightarrow 6,\Big\} \\
d_1^{(4)}(1^-,2^+) &= \frac{\langle 1|(3+4)|2]\langle 2\,1\rangle}{[1|(3+4)|2\rangle[2\,1]}\,d_1^{(4)}(1^+,2^+) \\
&= \frac{2}{s_{34}s_{56}\langle 1\,2\rangle[1\,2]\,\langle 2|(3+4)|1]^2} \\
&\quad\times\Big([4\,2]\langle 2|(3+4)|1]\langle 1\,5\rangle - [4\,1]\langle 1|(3+4)|2]\langle 2\,5\rangle\Big) \\
&\quad\times\Big([6\,1]\langle 1|(3+4)|2]\langle 2\,3\rangle - [6\,2]\langle 2|(3+4)|1]\langle 1\,3\rangle\Big)
\end{aligned}
$$

- Typical triangle:

$$
\begin{aligned}
c_1^{(0)}(1^-,2^+) &= 0 \\
c_1^{(2)}(1^-,2^+) &= \frac{1}{s_{34}s_{56}}\Big[-2\frac{\langle 1|(3+4)|2]}{\langle 2|(3+4)|1]^3}(s_{134}+s_{234})\langle 2\,3\rangle\langle 2\,5\rangle[1\,4][1\,6] \\
&\quad + \frac{1}{\langle 2|(3+4)|1]^2}\Big((s_{134}+s_{234})\big(\langle 1\,3\rangle\langle 2\,5\rangle[1\,4][2\,6] + \langle 1\,5\rangle\langle 2\,3\rangle[1\,6][2\,4]\big) \\
&\quad + \langle 2\,3\rangle[1\,6]\langle 5|(1+6)|4]\langle 1|(3+4)|2] - \langle 2\,5\rangle[1\,4]\langle 3|(1+4)|6]\langle 1|(3+4)|2]\Big) \\
&\quad - \langle 3\,5\rangle[4\,6]\frac{\langle 1|(3+4)|2]}{\langle 2|(3+4)|1]}\Big]
\end{aligned}
$$

Stability

- Note that the coefficients contain odd-looking denominators, but ones that can be recast into a more familiar form:

$$\frac{1}{\langle 1|(3+4)|2]^2} = \left(\frac{\langle 2|(3+4)|1]}{\langle 1|(3+4)|2]}\right)\frac{1}{\langle 1|(3+4)|2]\langle 2|(3+4)|1]} = \left(\frac{\langle 2|(3+4)|1]}{\langle 1|(3+4)|2]}\right)\frac{1}{s_{12}p_T^2}$$

  i.e. the same apparent singularities in the limit that $p_T(Z)\to 0$ as before.

- The singularities are tamed by rewriting in the 6-d box basis.
- Issue is completely removed for the LR amplitude.
- The LL amplitude contains higher-rank integrals, so some (milder) traces of the problem remain.
- Implementation good down to $p_T(Z)$ of 0.1 GeV.

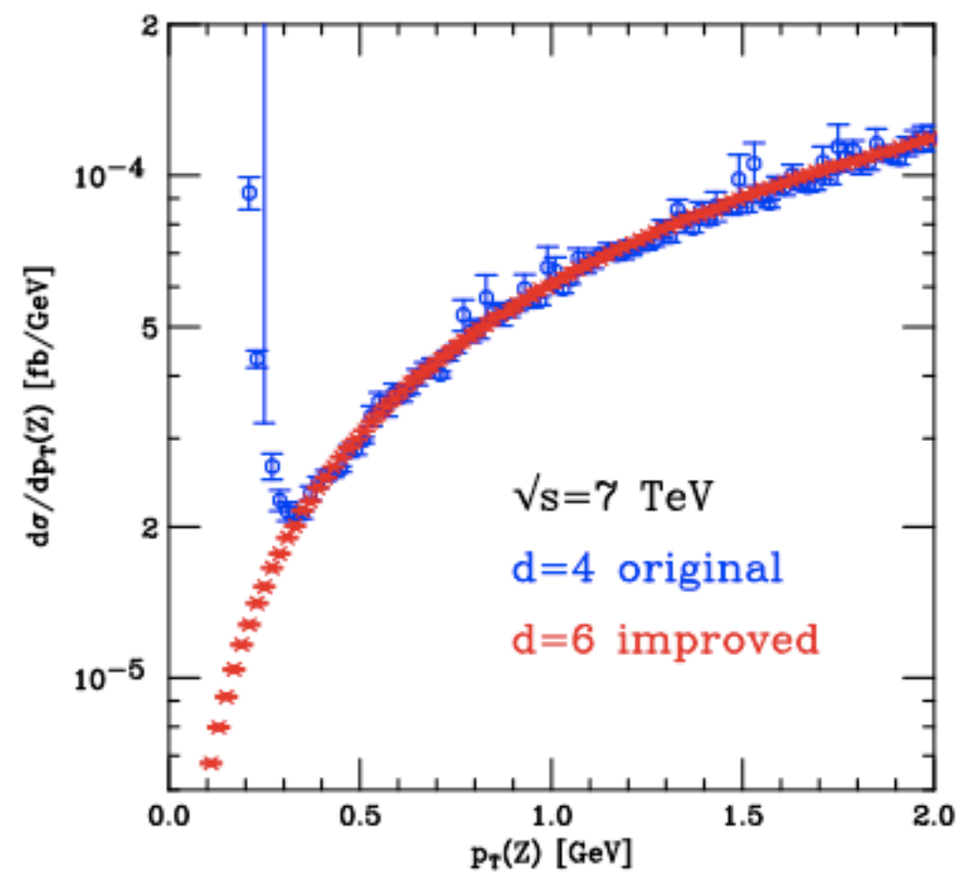

Enforced stability?

- Why not simply place a cut on the transverse momentum of the Z bosons?
- Outside the confines of the calculation, not very well motivated.
  - normal experimental cuts do not especially affect this region, since only lepton decay products are constrained.
- Surprisingly, fairly substantial contribution to the total cross section from the low p_T region.
- Cuts to enforce stability remove unacceptably-large chunk for the level of precision we desire.

cut @ 0.1 GeV → lose < 0.1%

cut @ 1 GeV → lose 0.3%

cut @ 7 GeV → lose 5-10%

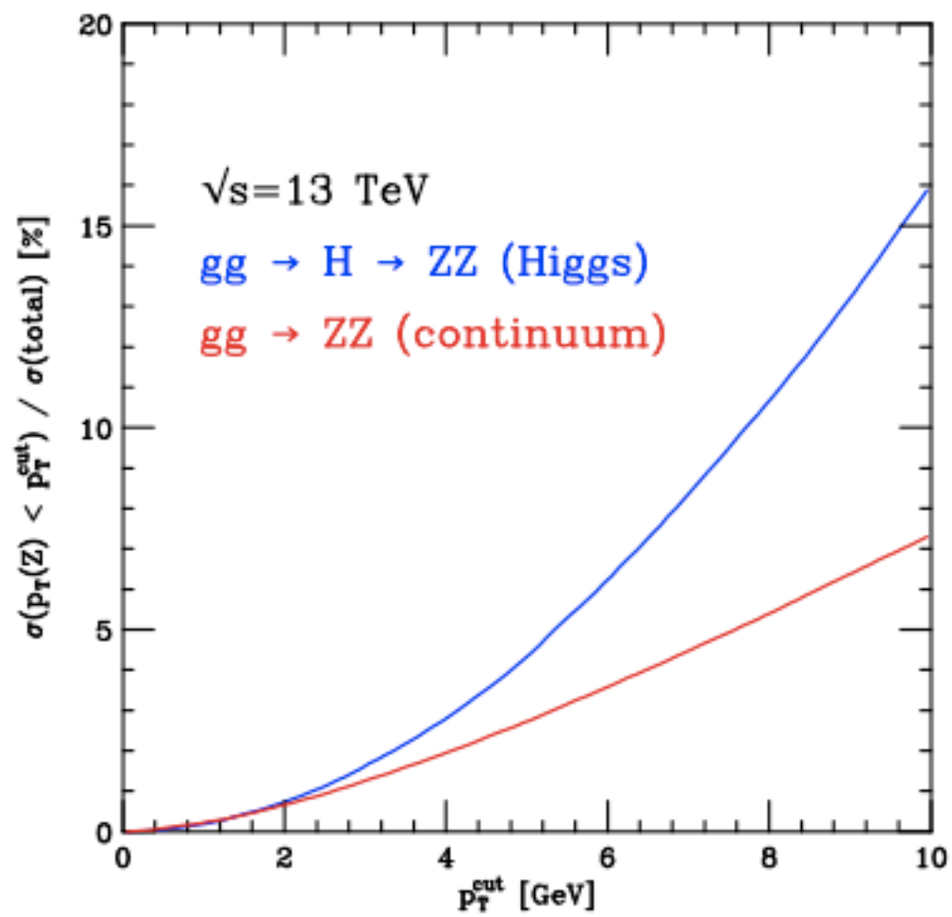

(essentially the same at other energies)

The result

- Cuts appropriate for CMS analysis of full data-set.

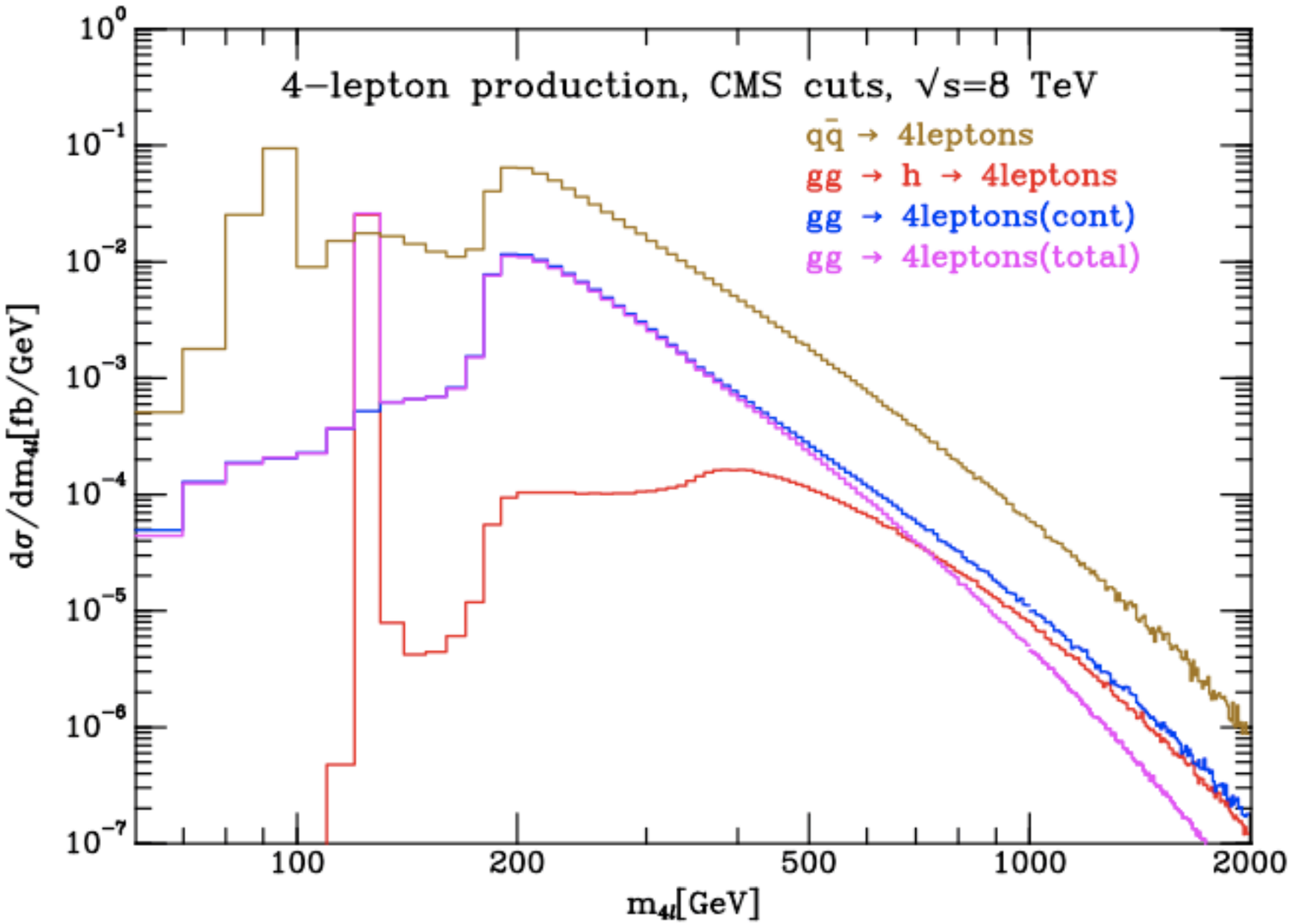

- Continuum ($q\bar{q}$) background 1-2 orders of magnitude larger throughout most of range.
- Effect of destructive interference clear for high m_{4l}.
- Difficult to observe effect (in the SM) since so little rate there.

More detail

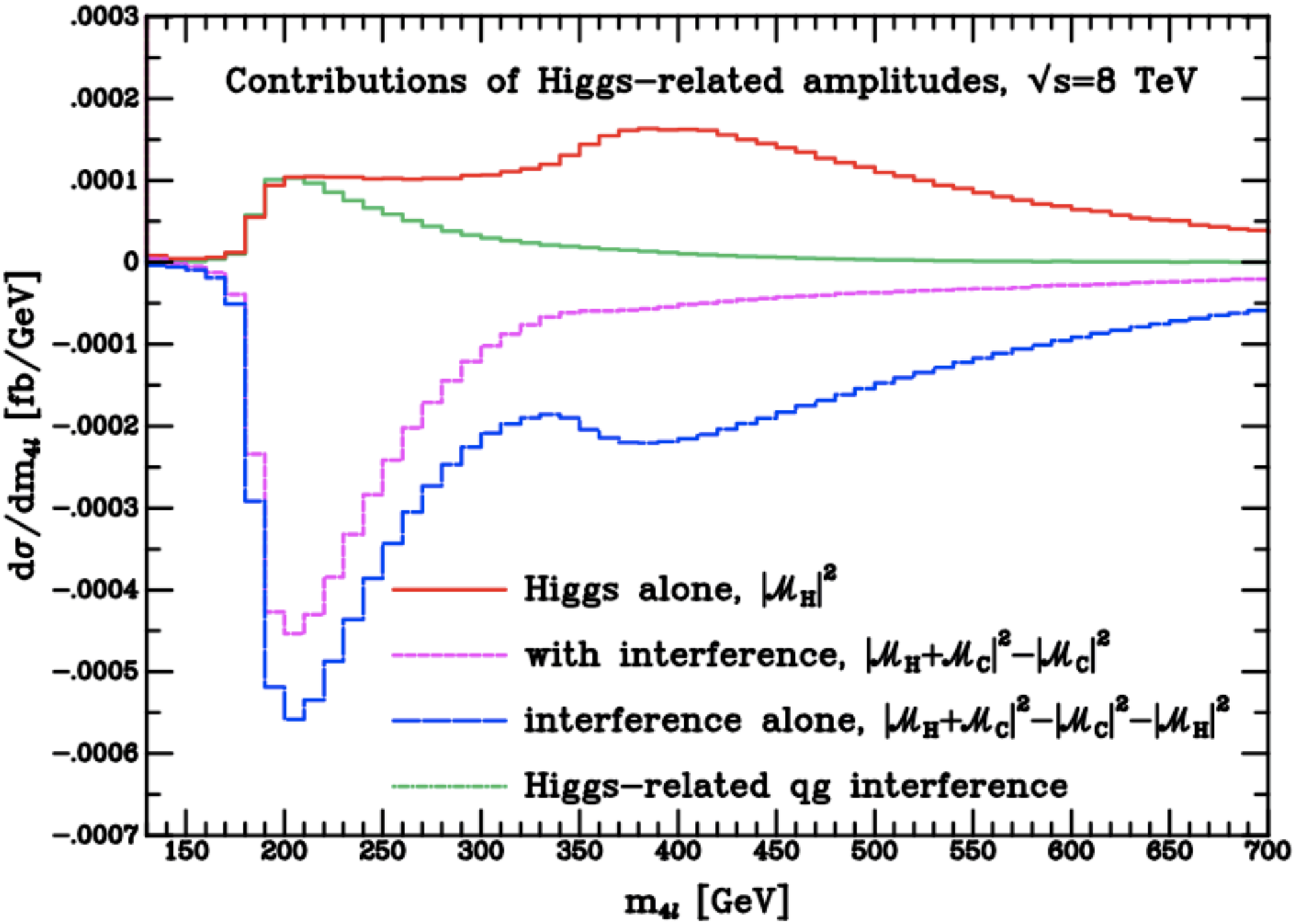

"qg interference" not so important

Cannot describe off-peak region without proper treatment of interference

By the numbers

Energy	PDF	σ^H_{peak}	$m_{4\ell} > 130$ GeV σ^H_{off}	$m_{4\ell} > 130$ GeV σ^I_{off}	$m_{4\ell} > 300$ GeV σ^H_{off}	$m_{4\ell} > 300$ GeV σ^I_{off}
7 TeV	MSTW	0.203	0.025	-0.053	0.017	-0.025
	CTEQ	0.192	0.021	-0.047	0.015	-0.021
8 TeV	MSTW	0.255	0.034	-0.073	0.025	-0.036
	CTEQ	0.243	0.031	-0.065	0.022	-0.031
13 TeV	MSTW	0.554	0.108	-0.215	0.085	-0.122
	CTEQ	0.530	0.100	-0.199	0.077	-0.111

- Define peak region and two (overlapping) off-shell regions.
- Effect of Higgs-induced diagrams on off-shell cross sections slightly larger at 13 TeV.
  - also, grows faster than competing $q\bar{q}$ background.
- Some variation of absolute cross sections with pdfs, but ratio (off-shell)/(peak) rather stable.

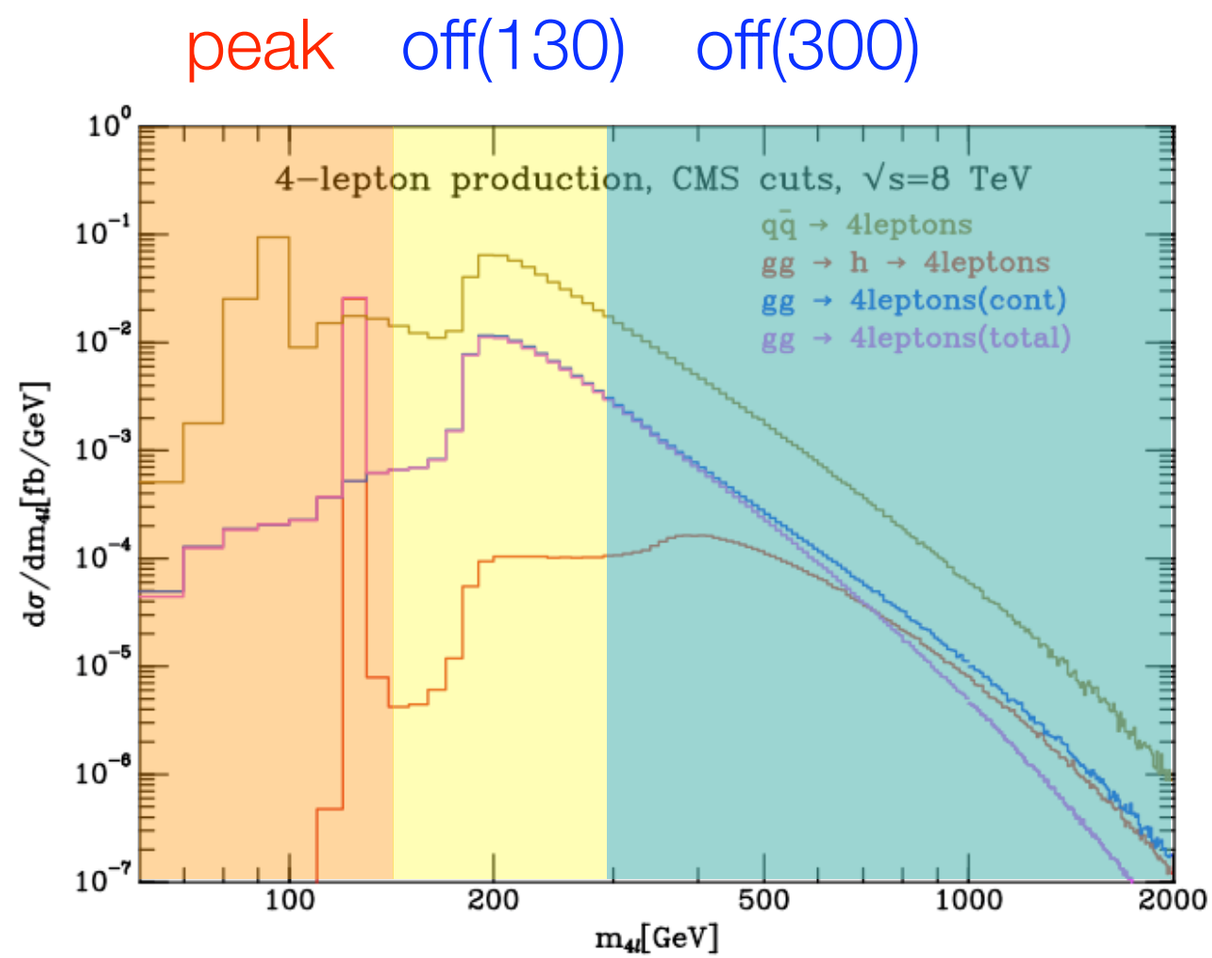

Relationship to the width

- Now in a position to use the ratio of the cross sections to probe the width.

$$\frac{\sigma_{off}^{H+I}(m_{4\ell} > 130\ \text{GeV})}{\sigma_{peak}^{H}} = 0.133\left(\frac{\Gamma_H}{\Gamma_H^{SM}}\right) - 0.286\sqrt{\frac{\Gamma_H}{\Gamma_H^{SM}}}$$

$$\frac{\sigma_{off}^{H+I}(m_{4\ell} > 300\ \text{GeV})}{\sigma_{peak}^{H}} = 0.098\left(\frac{\Gamma_H}{\Gamma_H^{SM}}\right) - 0.141\sqrt{\frac{\Gamma_H}{\Gamma_H^{SM}}} \qquad \text{(@ 8 TeV)}$$

- Note the importance of the second term that is necessary to describe the interference contribution (neglected in discussion earlier).
- Repeat analysis of Caola and Melnikov: directly use CMS results on H→ZZ taken at 7 and 8 TeV for robustness.
  - normalize to the peak cross section to obtain prediction for number of off-shell events.
  - compare this number with the observed data.

Expectation in CMS data

Channel	4e	4μ	$2e2\mu$	4ℓ
ZZ background	6.6 ± 0.8	13.8 ± 1.0	18.1 ± 1.3	38.5 ± 1.8
Z+ X	2.5 ± 1.0	1.6 ± 0.6	4.0 ± 1.6	8.1 ± 2.0
All background expected	9.1 ± 1.3	15.4 ± 1.2	22.0 ± 2.0	46.5 ± 2.7
$m_H = 125$ GeV	3.5 ± 0.5	6.8 ± 0.8	8.9 ± 1.0	19.2 ± 1.4
$m_H = 126$ GeV	3.9 ± 0.6	7.4 ± 0.9	9.8 ± 1.1	21.1 ± 1.5
Observed	16	23	32	71

CMS PAS HIG-13-002

Combination of 7 and 8 TeV data

- Obtain theoretical prediction by accounting for different luminosities and slightly different formulae at the two energies:

$$N^{4\ell}_{off}(m_{4\ell} > 130 \text{ GeV}) = 2.78\left(\frac{\Gamma_H}{\Gamma_H^{SM}}\right) - 5.95\sqrt{\frac{\Gamma_H}{\Gamma_H^{SM}}}$$

$$N^{4\ell}_{off}(m_{4\ell} > 300 \text{ GeV}) = 2.02\left(\frac{\Gamma_H}{\Gamma_H^{SM}}\right) - 2.91\sqrt{\frac{\Gamma_H}{\Gamma_H^{SM}}}$$

(expected Higgs events in total CMS data)

- Somewhat different from original Caola-Melnikov analysis:
  - choice of scale, use of gg2VV that inadvertently contained $p_T(Z)$ cut.

Comparison: indicative constraints

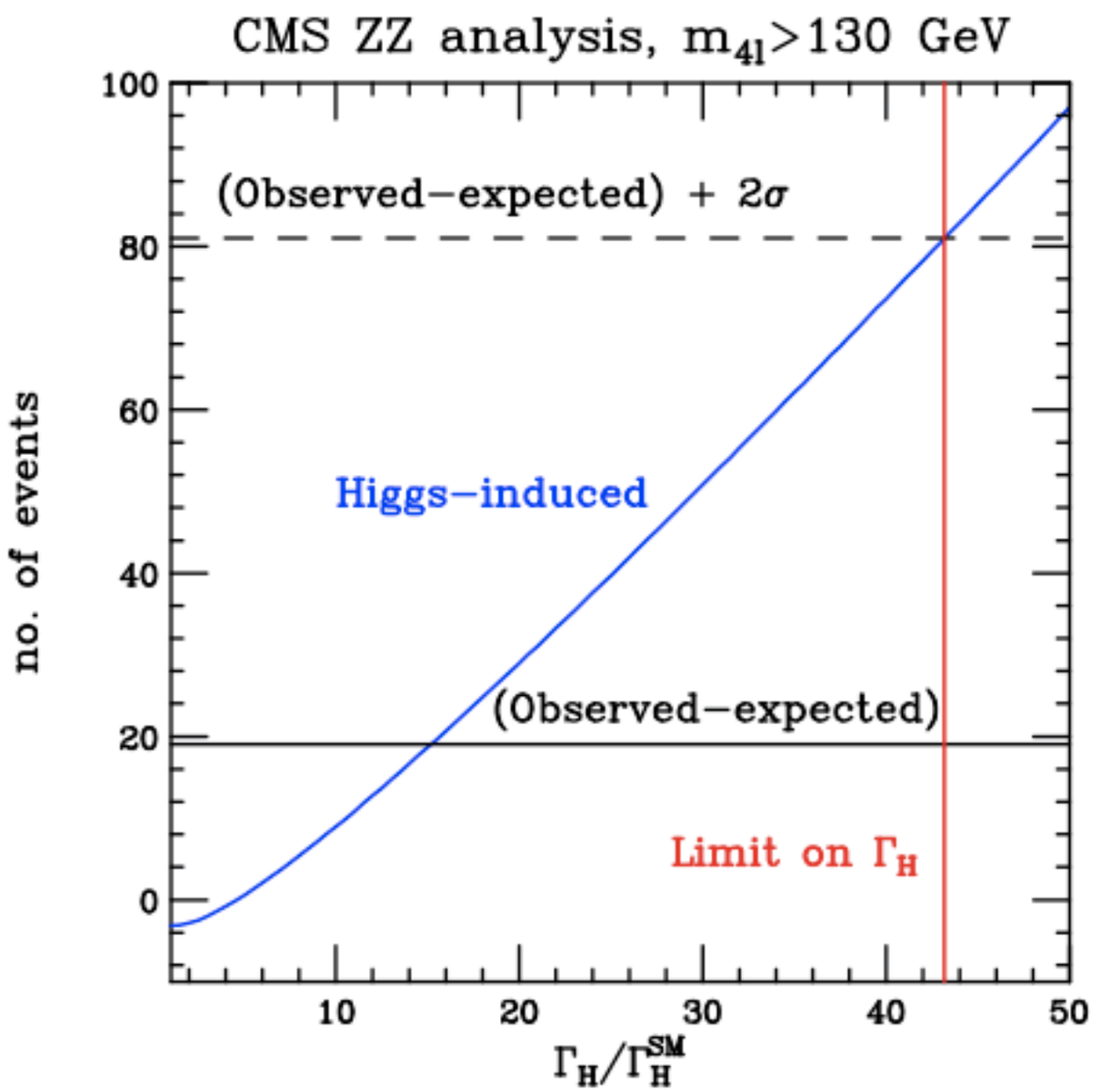

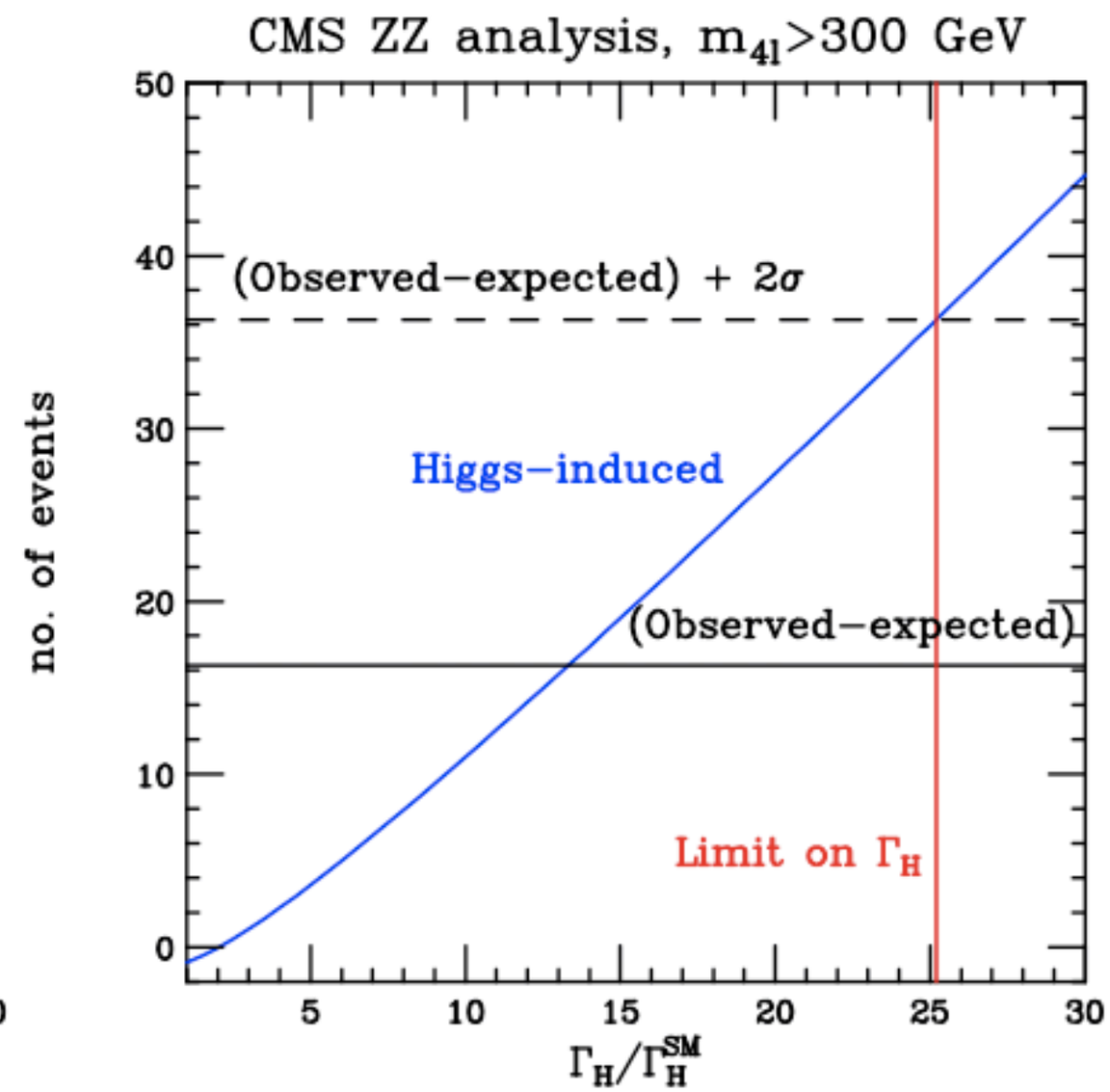

expected (no H): 432 ± 31

$$\Gamma_H < 43.2\,\Gamma_H^{SM} \text{ at } 95\% \text{ c.l.}$$

expected (no H): 71 ± (10?)

$$\Gamma_H < 25.2\,\Gamma_H^{SM} \text{ at } 95\% \text{ c.l.}$$

Matrix element method improvements

- Cut-and-count is the simplest approach and should improve substantially with more data.
- Meanwhile, use more kinematic information with a matrix element method.

Giele, Williams, JC; 1204.4424

Data event φ

↓

Probability of event under different hypotheses

(integration over equivalent longitudinal boosts to map to 2→4 phase space)

$$P_{LO}(\phi) = \frac{1}{\sigma_{LO}} \sum_{i,j} \int dx_1 dx_2 \, \delta(x_1 x_2 s - Q^2) f_i(x_1) f_j(x_2) \hat{\sigma}_{ij}(x_1, x_2, \phi)$$

↙ ↓ ↘

$P_{q\bar{q}}$	:	$q\bar{q}$ initiated background.
P_{gg}	:	gg initiated pieces, including Higgs signal, box diagrams and interference.
P_H	:	gg initiated Higgs signal squared.

- Compute discriminant to understand which hypothesis preferred:

$$D_S = \log\left(\frac{P_H}{P_{gg} + P_{q\bar{q}}}\right)$$

Mock-up of CMS

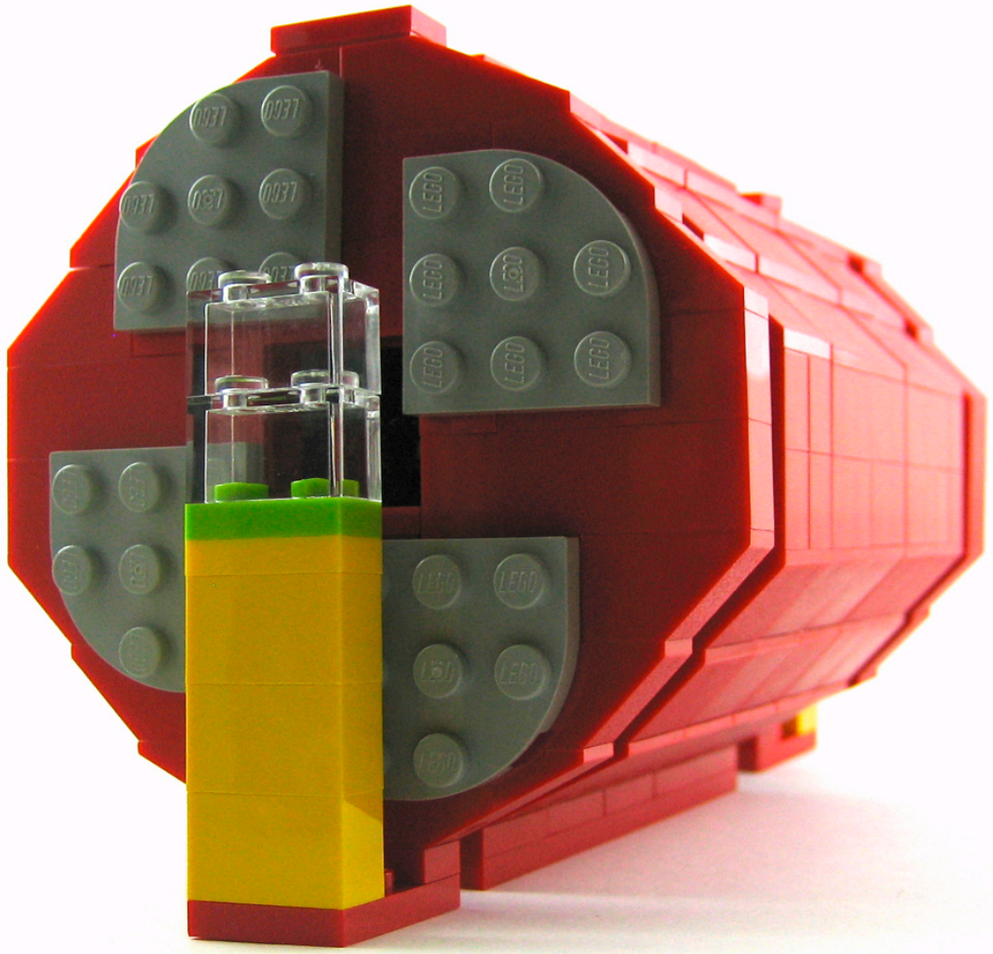

http://www.physics.umd.edu/rgroups/hep/LegoCMS/CMSmini/index.html

- Cannot use real CMS data!
- Instead our “data” obtained as follows:
  - POWHEG+Pythia for dominant $q\bar{q}$ background
  - Higgs signal + interference from our calculation, interfaced with the same Pythia shower
  - smear lepton p_T with a Gaussian of width 0.5 GeV (~ CMS-like)
- Obviously no substitute for in-situ analysis with full detector simulation and actual data.

MEM analysis

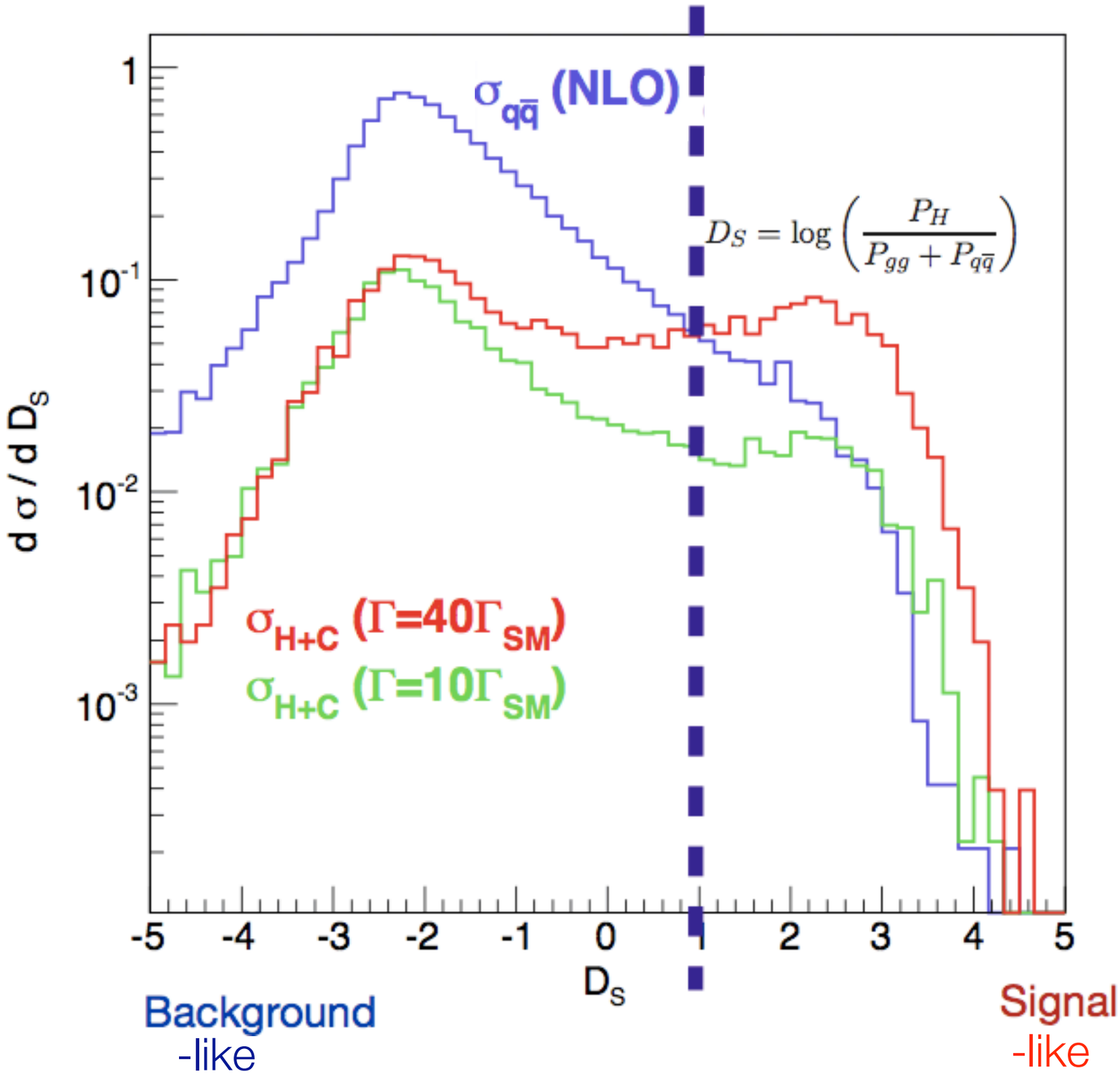

Discriminant effectively isolates gluon-related contributions from $q\bar{q}$ backgrounds.

- a simple cut on D_s would suffice

Number of events passing cut sensitive to the width.

Using an analysis that roughly mimics the CMS results found before, a cut D_s>1 finds:

$$\Gamma_H < (15.7\ ^{-2.9}_{+3.9})\ \Gamma_H^{SM} \text{ at } 95\% \text{ c.l.}$$

WW

- The ZZ channel is convenient: well-measured leptons allow the Higgs boson lineshape to be mapped out and peak/off-shell regions directly identified.
- However, exact mapping of lineshape is not crucial, just need well-separated regions corresponding to on- and off-resonance.
- Try to play the same game in WW channel:

$$gg \to W^+W^- \to e^+\mu^-\nu_e\bar{\nu}_\mu$$

- As proxy for invariant mass, use transverse mass of expected WW system:

$$M_T^2 = (E_T^{miss} + E_T^{\ell\ell})^2 - |\mathbf{p}_T^{\ell\ell} + \mathbf{E}_T^{miss}|^2$$

- Some features washed out, but clear separation between peak and tail remains.

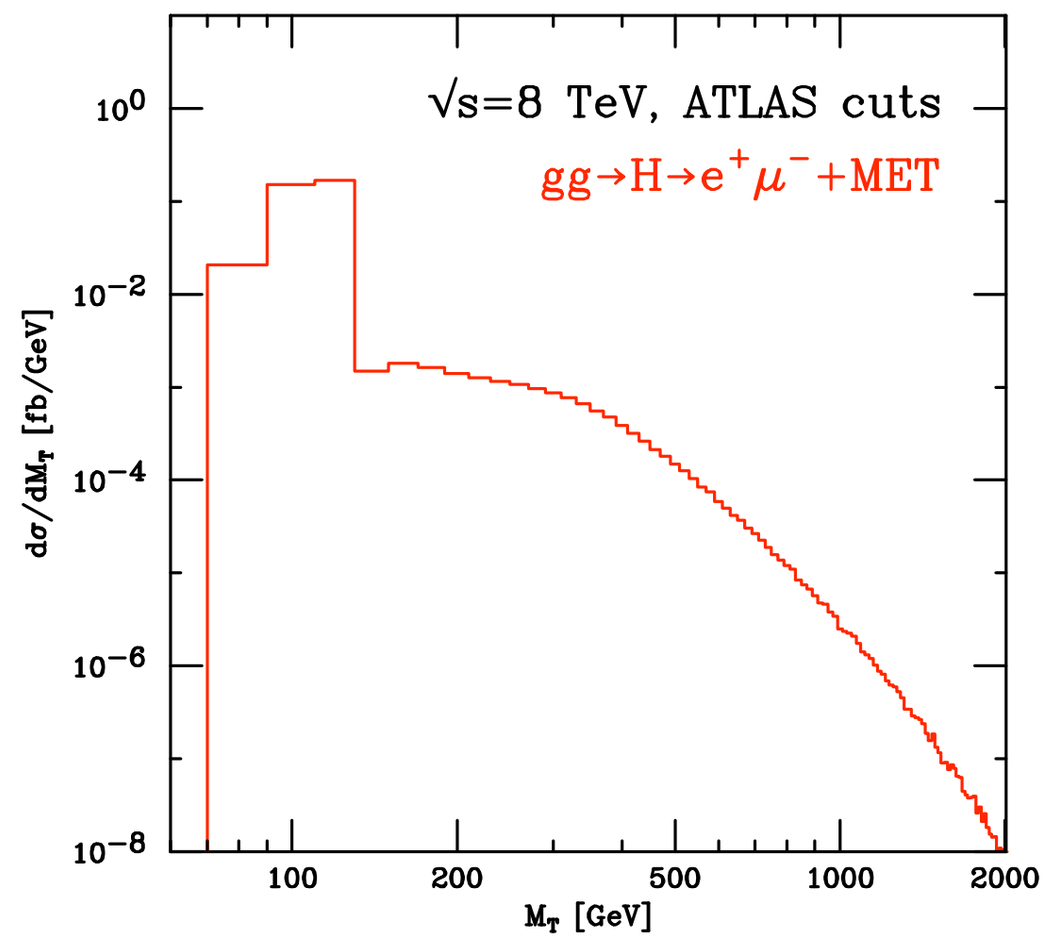

WW vs ZZ

- Advantages:
  - threshold for two real W's much closer than for two real Z's
  - branching ratio into leptons also larger
  - combined, two orders of magnitude more events:

$$\mathrm{Br}(H \to WW) \times \mathrm{Br}(W \to \ell\nu)^2 = 2.7 \times 10^{-3}$$
$$\mathrm{Br}(H \to ZZ) \times \mathrm{Br}(Z \to \ell^+\ell^-)^2 = 3.2 \times 10^{-5}$$

- Disadvantages:
  - much less clean so many more backgrounds
  - particularly, top-related that require a jet-veto to control
  - as a result, even observation of the Higgs boson in this channel alone not yet confirmed.

Status of theory for gg→WW

- Continuum similar to gg→ZZ, but additional single-resonant diagrams.
- Massless loops of quarks a trivial subset of previous calculation.
- Third generation more tricky: compute for $m_t > 0$, $m_b = 0$. Compact analytic results.

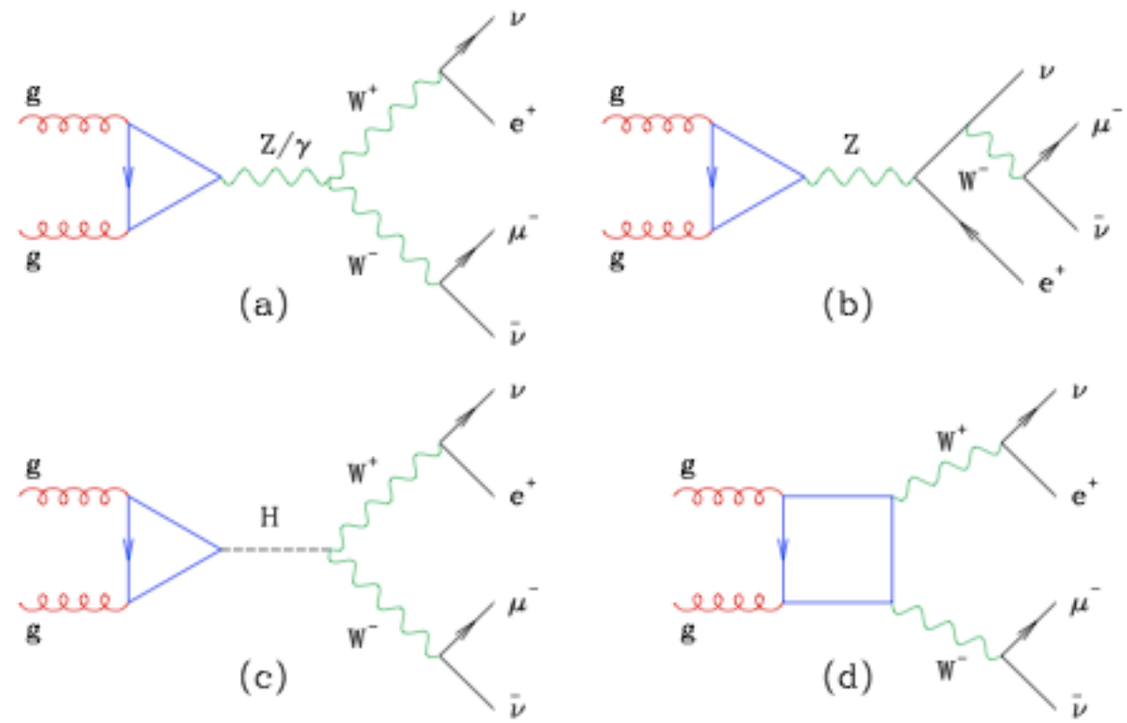

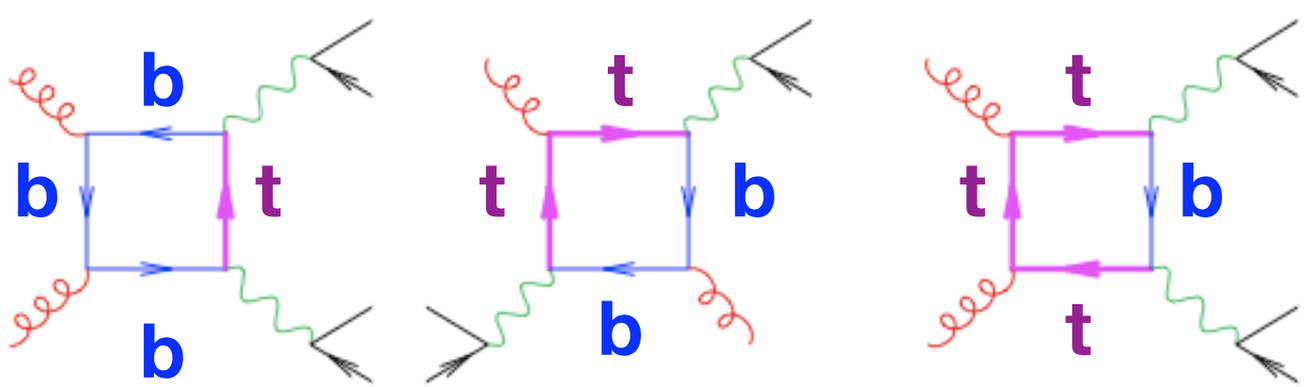

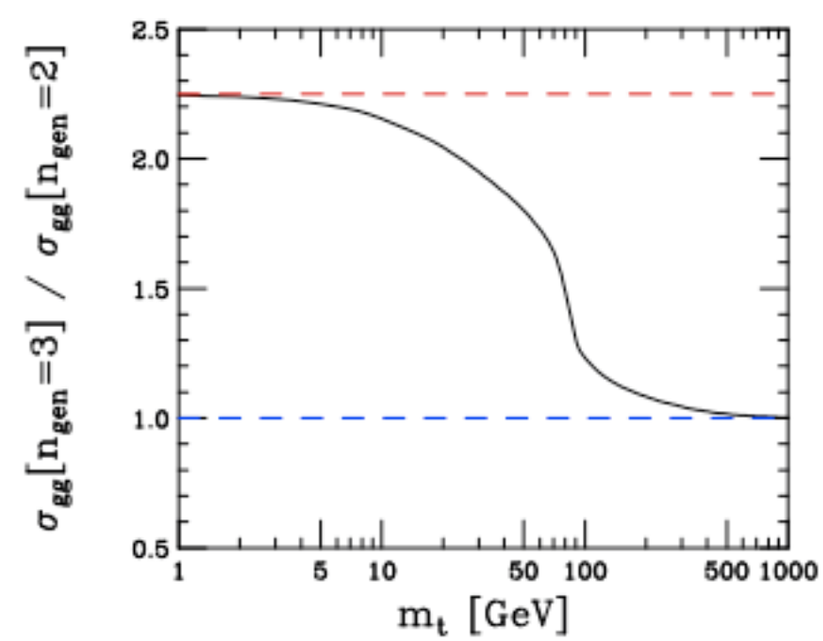

- Previously used to study effect of interference on search strategy. Williams, Ellis, JC; 1107.5569

Comparison with ATLAS cuts

- As well as a jet veto to handle top backgrounds, analysis must apply specific cuts to favour the Higgs signal over the $q\bar{q}$ background.

$$m_{\ell\ell} < 50 \text{ GeV}, \quad \Delta\phi_{\ell\ell} < 1.8$$

ATLAS-CONF-2013-030

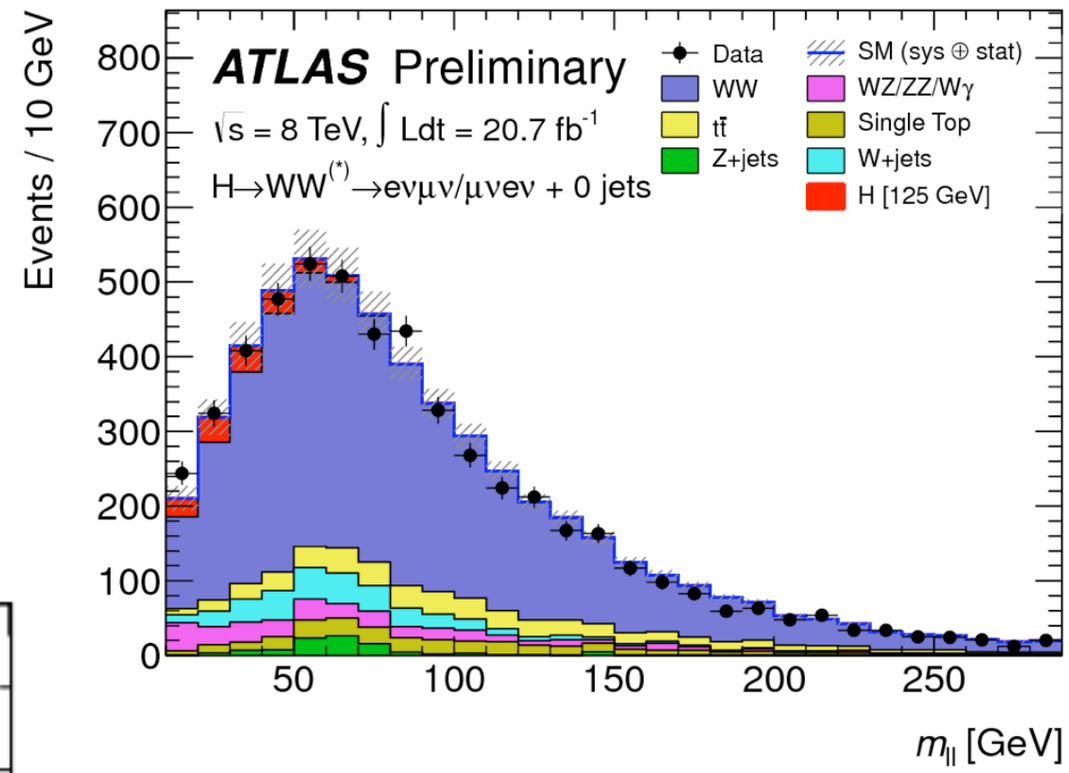

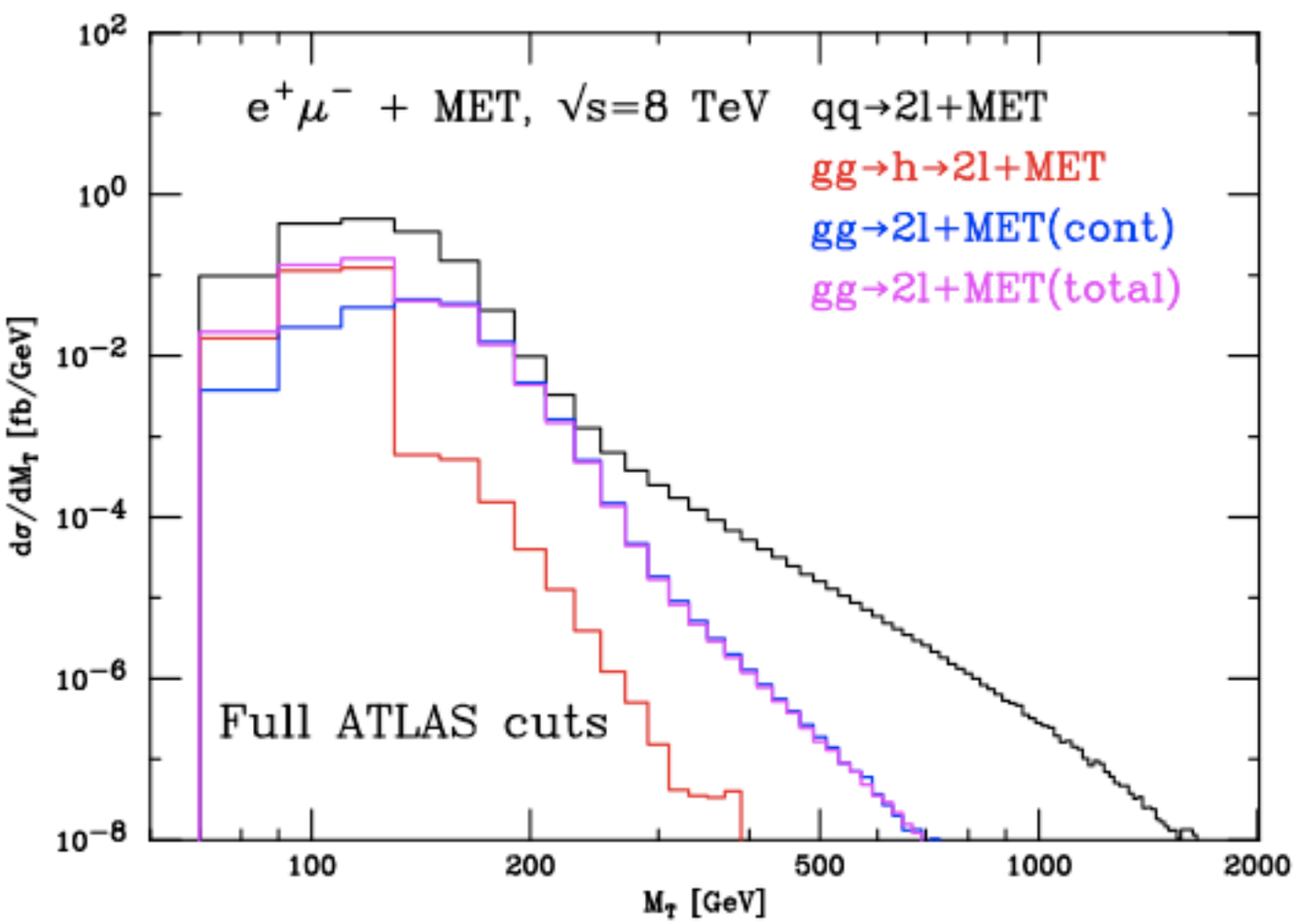

- Excellent strategy for observing this channel, i.e. peak cross section.
- No tail left to play with for width analysis.

Recovering the tail

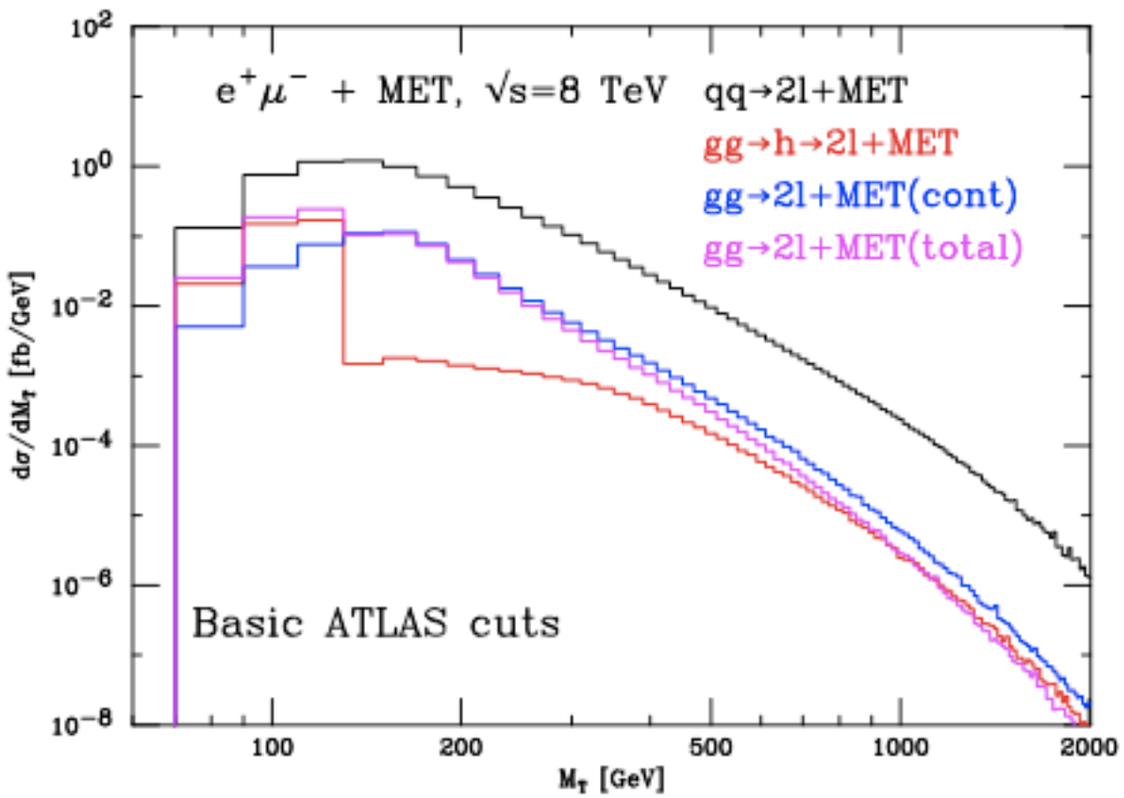

keep no dilepton cuts

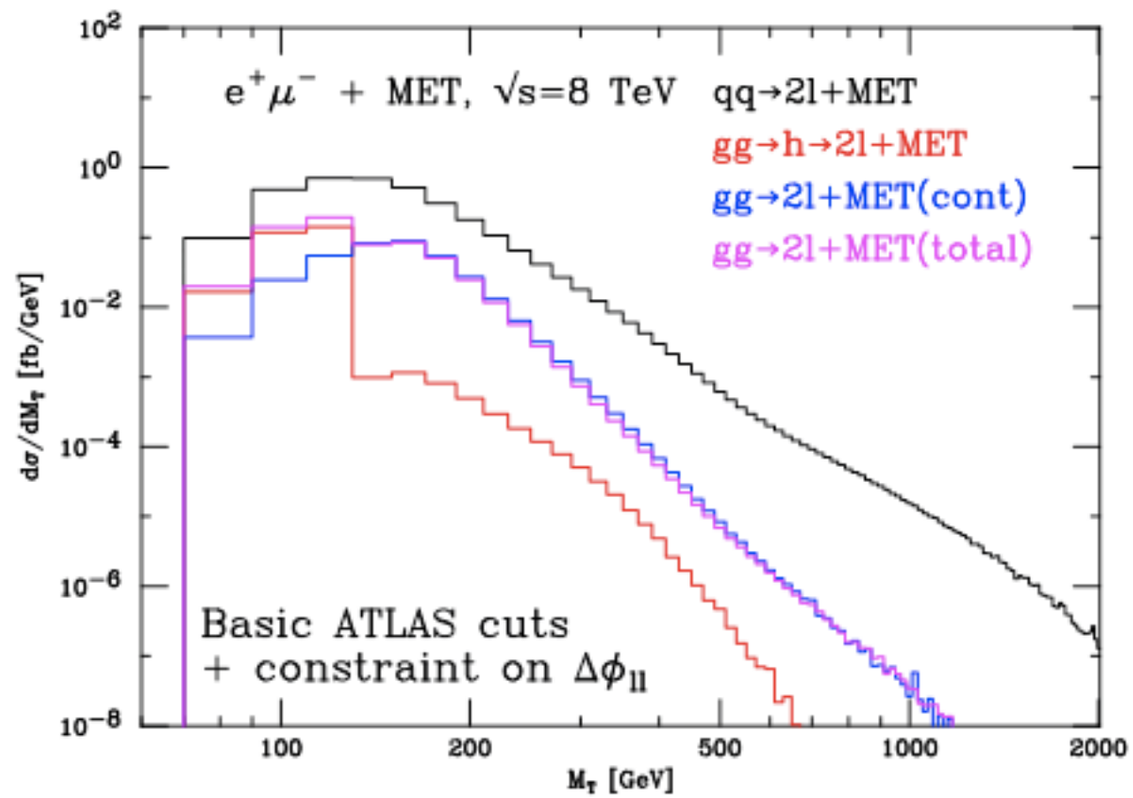

keep only Δφ cut

- With no dilepton cuts, same features observed as before
  - destructive effect of interference at high M_T
- With only Δφ cut, tail remains and still good suppression of $q\bar{q}$ background.

Estimate of sensitivity

- Requires even more of a leap of faith than ZZ analysis
  - ATLAS uncertainties only presented in the resonance region.
- Extrapolation, estimation of backgrounds, systematic uncertainties, ...
- Best sensitivity with basic cuts in the region with M_T > 300 GeV.

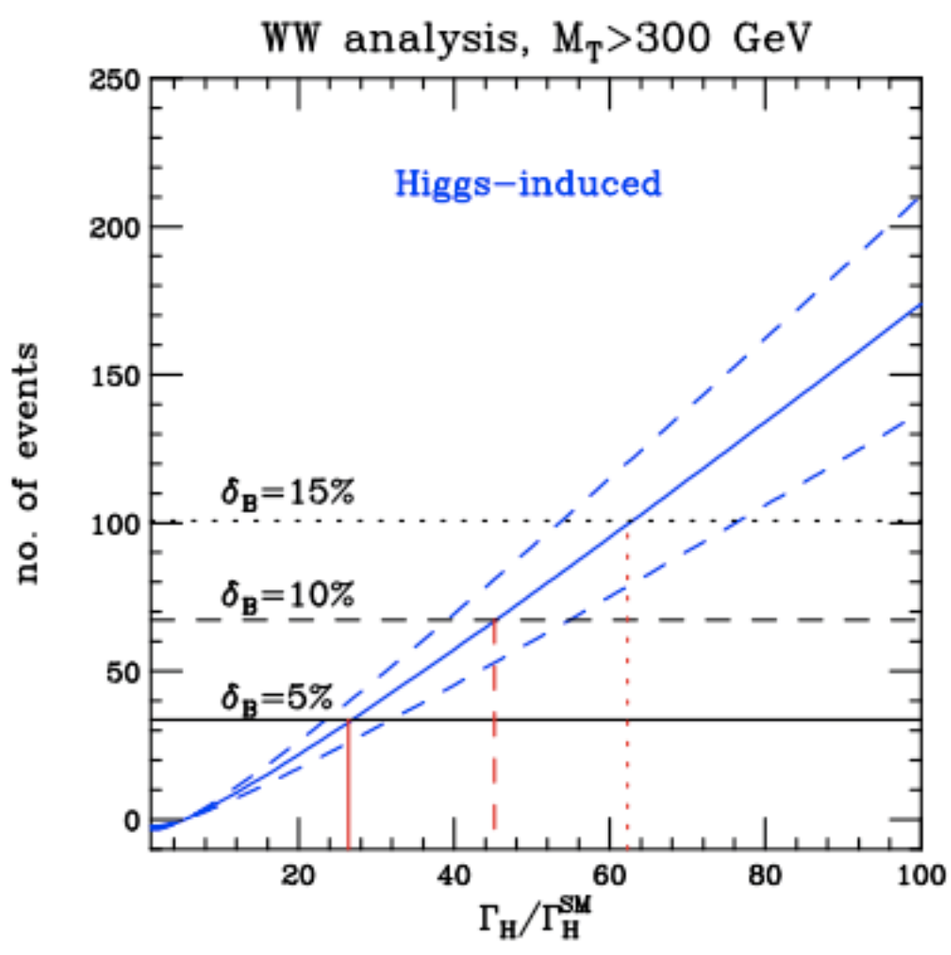

- <B>=336 events
- Try to be conservative by using systematic uncertainty on theory and your choice of experimental systematic uncertainties.

$$\Gamma_H < 45^{+9}_{-7}\,\Gamma_H^{SM}$$

- Different flavour, 20 fb^{-1}, δ_B=10%.

Other approaches

- Direct: interferometry in diphoton decay; interference induces change in diphoton mass distribution that depends on the width.

  Dixon, Li; 1305.3854

- Require precise measurement of mass shift between ZZ and diphoton channels.

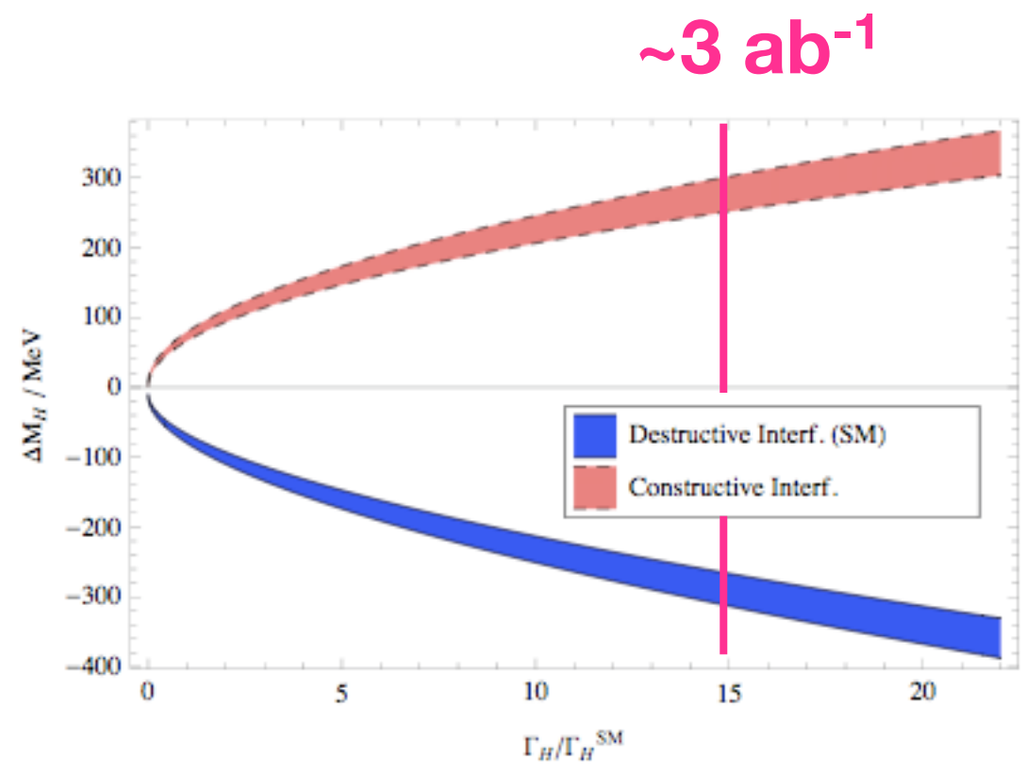

- Indirect: global coupling fits; assume either that the coupling to W,Z takes the SM value, or is bounded by reasonable theoretical assumptions.

  Dobrescu, Lykken; 1210.3342

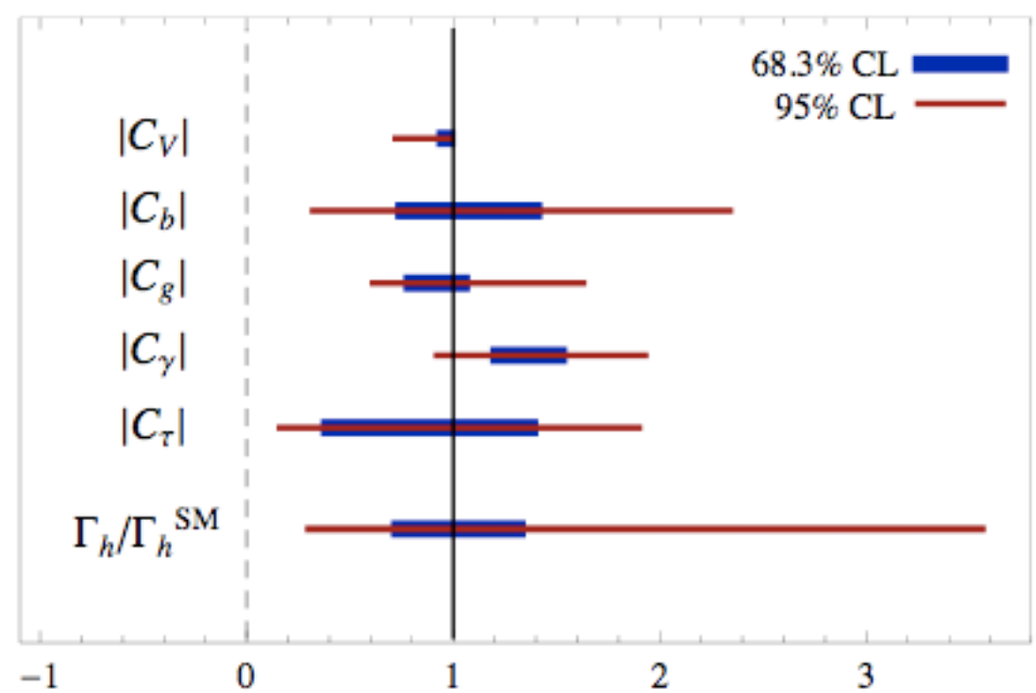

Comparison of direct constraints

LHC now

Method	Measured quantity	Γ_H [MeV]	$\Gamma_H/\Gamma_H^{\rm SM}$
CMS-PAS-HIG-13-016	Width $\times$ resolution	< 6900	< 1600
1305.3854 (Dixon-Li)	Mass shift in $\gamma\gamma$, $\Delta m_H \sim 1$ GeV	< 800	< 200
1312.1628 (CEW)	Ratio WW, $m_T > 130$, 300 GeV, MEM	$< 500, 180$	$< 125, 45$
1311.3589 (CEW)	Ratio ZZ, $m_{4\ell} > 130$, 300 GeV	$< 170, 100, 60$	$< 43, 25, 15$

LHC future

Method	Measured quantity	Γ_H [MeV]	$\Gamma_H/\Gamma_H^{\rm SM}$
Snowmass estimate 3 ab^{-1}	Width $\times$ resolution	< 200	< 50
1305.3854 (Dixon-Li) 3 ab^{-1}	Mass shift in $\gamma\gamma$, $\Delta m_H \sim 100$ MeV	< 60	< 15
1307.4935 (CM) 3 ab^{-1}	Ratio ZZ, $m_{4\ell} > 130$, 300 GeV	$< 40, 20$	$< 10, 5$

- CM method, i.e. ratio of off- and on-peak cross sections, looks most powerful;
- .... for now. Plenty of time for refinements and new ideas.

Conclusion

- Direct bounds on the Higgs boson width at the LHC are hard to come by.
- The approach presented here relies on comparisons of ZZ and WW cross sections in regions close to, and far above, the Higgs resonance.
- This method (“ Caola-Melnikov”) therefore requires precise predictions for these final states, particularly in the gg channel.
- Hence, presented re-calculation of the gg 1-loop amplitudes that produces results in compact analytic form. Resulting code is numerically stable.
  - available in MCFM v6.8
  - can produce LHE events for subsequent showering
- Method appears viable and motivates future refinements
  - impact of other final states ($\ell\ell\nu\nu$, $\ell\ell jj$) should be studied too
  - calculation of gg contribution beyond this order; important to know NLO QCD (normalization uncertainty) and EW (tails of distributions).